SYNTHESIS AND ENGINEERING STUDIES OF BIOBASED AND BIODEGRADABLE-COMPOSTABLE POLYMERS

By

Badal Girish Lodaya

A THESIS

Submitted to
Michigan State University
in partial fulfillment of the requirements
for the degree of

Chemical Engineering- Master of Science

2024

ABSTRACT

In this thesis, the focus is on Polylactide (PLA) based polymers, recognized as the leading 100% biobased resin globally. These polymers align with the Circular Economy model proposed by the Ellen MacArthur Foundation, offering both composting and recycling as viable end-of-life options. PLA is commercially produced by transforming lactic acid into lactide, followed by polymerization. The unique stereochemistry of PLA molecules significantly influences manufacturing processes, performance characteristics, and overall processability. Despite its importance, the role of stereochemistry in shaping PLA's product performance and applications is often overlooked and not thoroughly understood. The present work discusses stereo-complex PLA using reactive extrusion to improve the mechanical performance of thermoplastic PLA matrix. It also focuses on polymerization of meso-PLA and further modification of Poly (meso-lactide) and commercial PLA grades for applications in paper- coating. Lastly, reactive extrusion is emphasized as a continuous and facile method for synthesis of PCL and PLA. The overall aim of the thesis is to focus on utilization of PLA in different domains of application through synthesis or modification using twin-screw extruder as a facile approach.

For all the people who believe in me,
This thesis is dedicated to you.

ACKNOWLEDGEMENTS

I would like to thank Dr. Ramani Narayan, my advisor and mentor for guiding me through my research journey at Michigan State University and preparing me for the world outside the university. I would also like to thank my colleagues at Michigan State University and Natur-Tec for helping me learn and grow in the field of polymer science and for providing me with a valuable helping hand in carrying out work for this thesis.

I thank my alma-mater, ICT Mumbai, for providing me with the fundamental base and knowledge of Chemical Engineering. Lastly, I would like to thank my friends and family members for their infinite support and continuous motivation.

TABLE OF CONTENTS

RATIONALE

A recent collaborative technical report from the World Economic Forum and the Ellen MacArthur Foundation projects that by 2050, the volume of plastics in the ocean will exceed that of fish [1]. Although this forecast may not provide an exact portrayal of 2050, it vividly highlights the critical concern of plastic waste that is currently prevalent (refer to **Figure 1**). In the last decade, the issue of plastic waste has gained prominence in both scientific and non- scientific circles [2][3]. Despite a nearly 20-fold surge in plastic production over the past 50 years, effective strategies to manage the resulting waste remain limited (as depicted in **Figure 1**). Present estimates indicate that only 14% of plastic waste undergoes recycling, while 40% ends up in landfills, 14% is incinerated or used for energy recovery, and a concerning 32% escapes into the environment [1]. The dispersion of such plastic waste has prompted investigations into microplastic formation in soil and marine environments, correlating with harmful effects on various organisms [4][5]. This alarming situation underscores the urgent need for the development of plastics that can be appropriately managed at the end of their useful life.

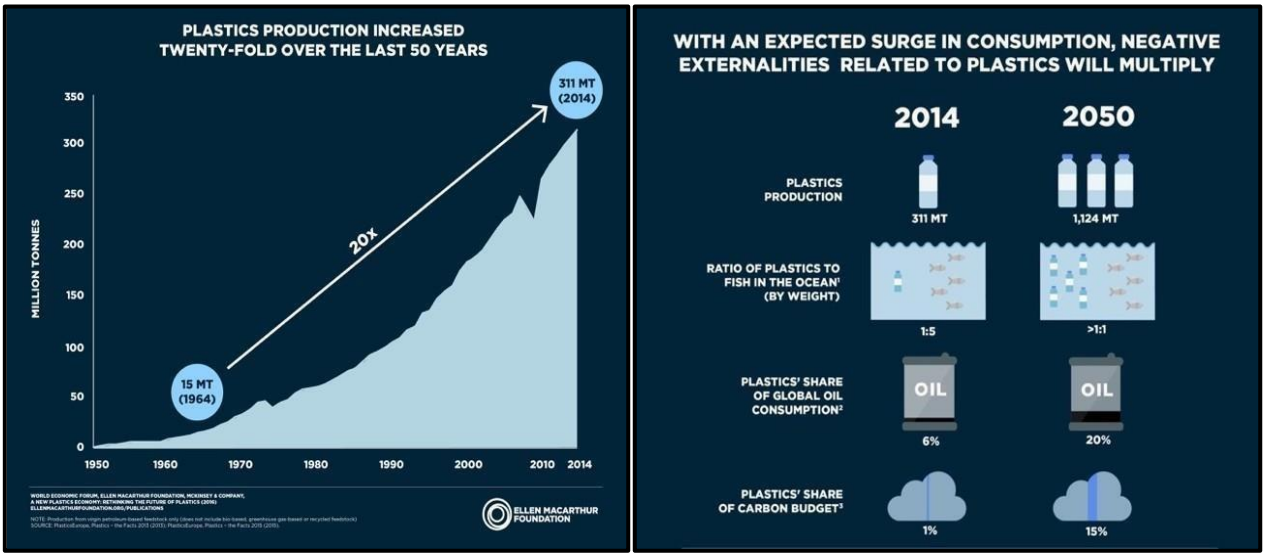

Figure 1: Increase in the production of plastics over the last 50 years (left), prediction of plastics waste for year the 2050 (right) [3]

According to IUPAC, biobased plastics or materials are derived wholly or partially from biomass, including plant, animal, and marine or forestry materials. These materials offer significant environmental benefits by reducing carbon footprint during production. Polylactic acid (PLA), a notable biobased plastic, is also biodegradable under controlled conditions like composting, presenting a viable end-of-life solution [4]. Consequently, PLA and similar materials hold promise in addressing the plastic waste issue by closing the production and use cycle (**Figure 2**). Despite abundant scientific literature on PLA synthesis and modification, few cost-effective strategies exist due to academic nature and scaling challenges [5].

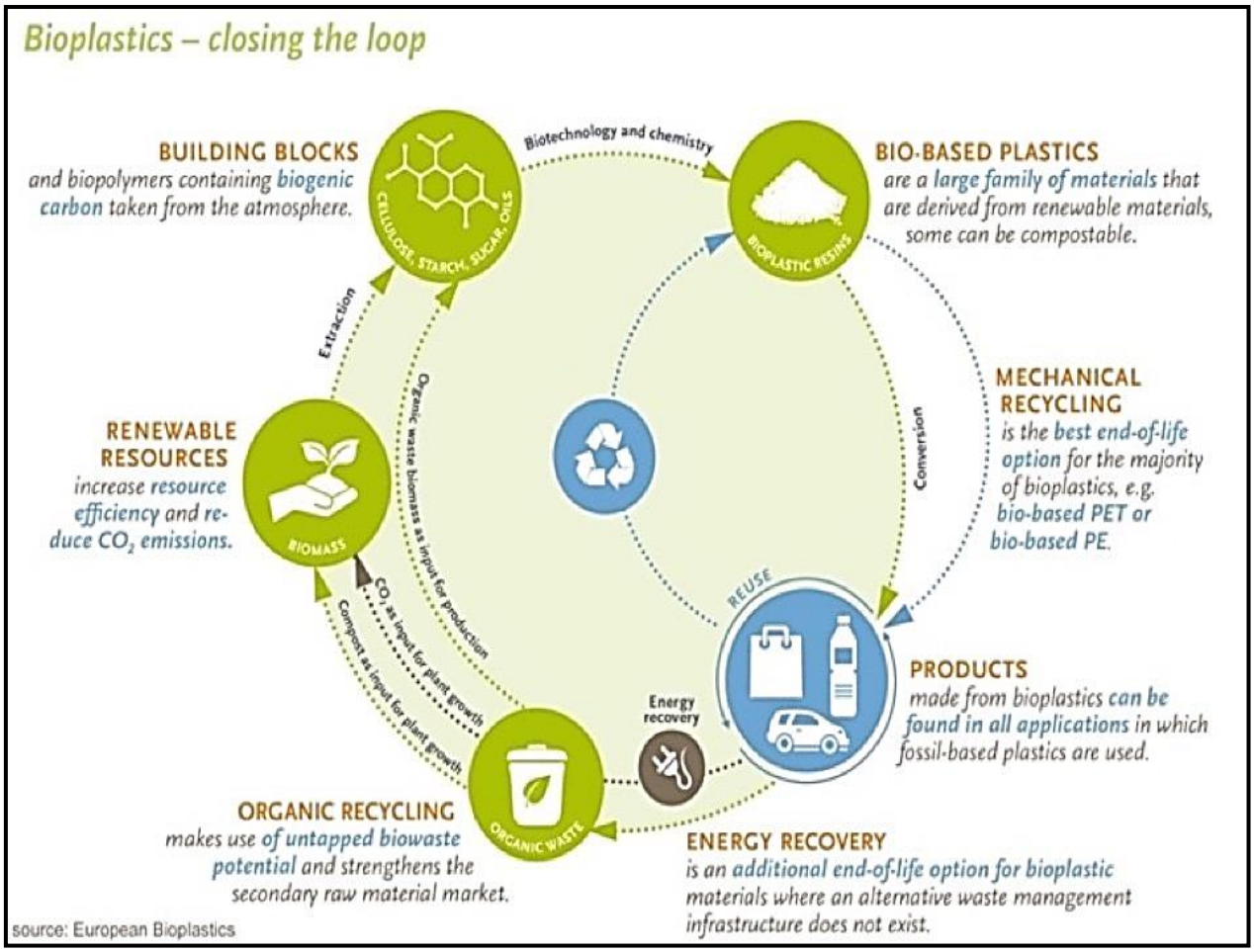

Figure 2: Closed-loop cycle showing the ideal path taken by biobased plastics (Image sourced from www.europeanbioplastics.org)

1.1 Polylactide (PLA)

PLA was initially synthesized in 1932 by Wallace Carothers at DuPont. The process involved heating lactic acid under a vacuum while eliminating the formed water vapor [6]. However, the outcome was characterized by low molecular weight and subpar mechanical properties. An alternative route to PLA synthesis involves utilizing lactide, the cyclic di-ester of lactic acid. Presently, the production of high molecular weight PLA is achieved through one of the subsequent approaches depicted in **Figure 3**[7]: (a) the ring-opening polymerization of lactide monomers, or (b) the polycondensation reaction of lactic acid, followed by an azeotropic distillation process employing a high-boiling solvent to enhance the equilibrium reaction. Cargill Inc. has successfully commercialized the former technique, while Mitsui Toatsu Chemicals has adopted the latter. A third method exploring the use of chain coupling agents to augment the initial PLA's molecular weight has been investigated, but its implementation remains limited due to factors like added expenses and the presence of unreacted impurities in the final product [8].

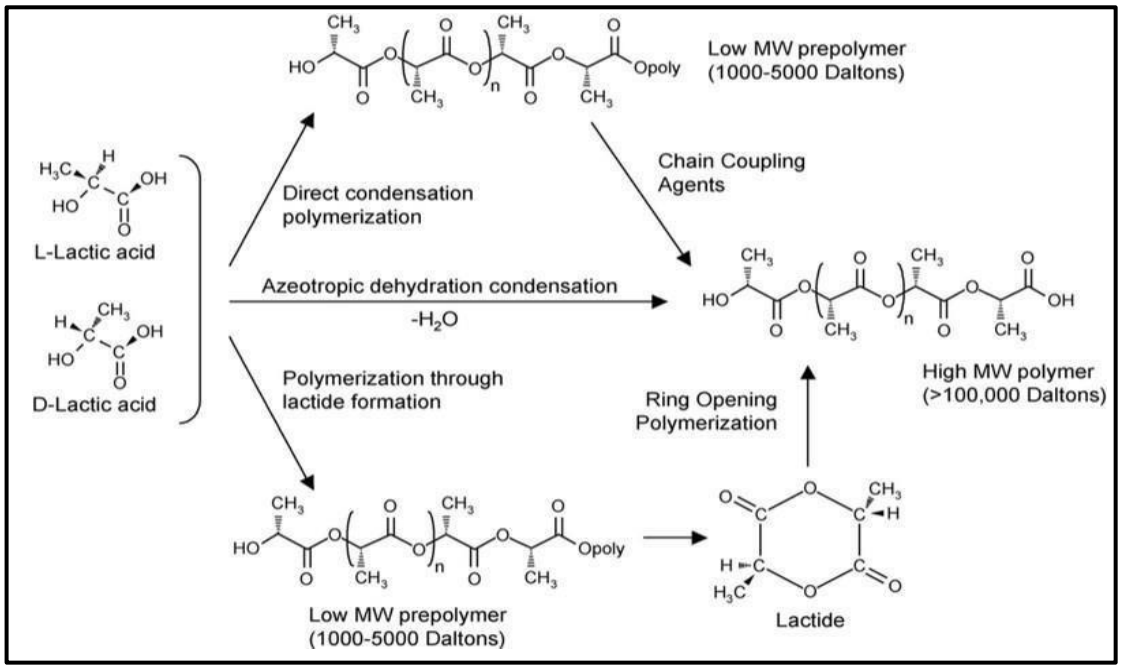

Figure 3: Various routes for the synthesis of PLA [9]

As shown in **Figure 4**, lactide exists in the form of three stereoisomers [8]: L-lactide, D-lactide and meso-lactide.

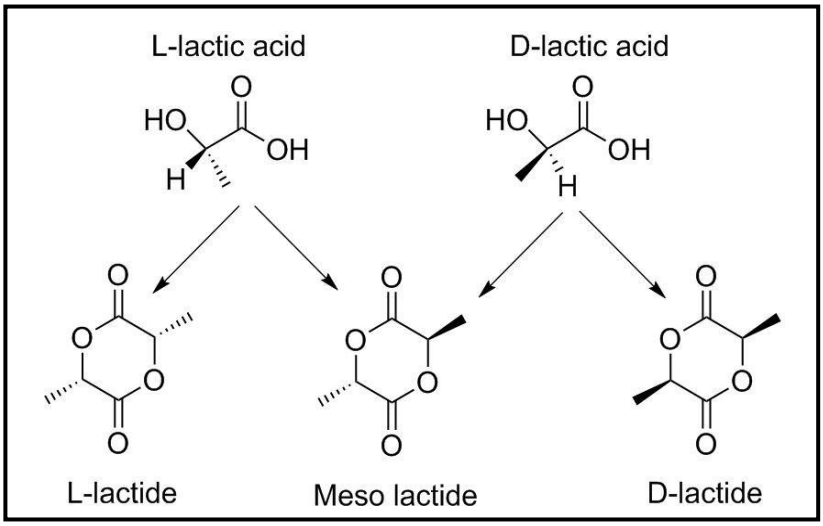

Figure 4: Stereoisomers of lactide

The stereochemical composition of polylactic acid (PLA), formed through the ring-opening polymerization of lactide monomers, significantly influences its properties such as melting point and crystallization rate. Pure poly (L- or D- lactide) typically exhibits a melting point around 180°C, decreasing with the presence of stereochemical impurities. While the glass transition temperature remains independent of stereochemical composition, ranging from 55 to 60°C, PLA's thermal degradation initiates at about 180 to 190°C due to chain scission.

PLA demonstrates mechanical properties comparable to polystyrene (PS), making it a potential eco-friendly substitute. However, its low toughness and elongation at break restrict certain applications. Regarding barrier properties, PLA outperforms PS in oxygen, carbon dioxide, and moisture permeability. Moreover, PLA's minimal migration of chemical species into packaged products qualifies it as "Generally Recognized as Safe" (GRAS) by the FDA.

Biodegradability studies indicate that PLA requires enzymatic degradation by specific microbes, as it undergoes breakdown into lower molecular weight oligomers in natural environments.

Despite its versatility in applications like packaging and biomedical implants, PLA faces limitations such as low toughness, slow crystallization rate, and poor melt strength, posing challenges for its widespread use. Efforts are ongoing to address these limitations through extensive research.

1.2 Reactive Extrusion (REX)

Extrusion-based systems offer an uninterrupted and cost-efficient approach to polymer processing. Reactive extrusion (REX) stands out as a highly adaptable method, suitable for a wide range of applications, including polymerization reactions, chemical enhancements involving grafting, branching, and functionalization reactions, as well as physical modifications like reactive blending and compatibilization [10][11].

Figure 5 illustrates the basic schematic of a REX process. Solid and liquid reactants are introduced through a feeder and an injection pump, respectively. The barrel, comprising individually heated blocks, contains screw elements responsible for both mixing and conveying. The final product exits the extruder through a die located at the barrel's end. The motor at the front of the assembly imparts torque to drive the screws. Extruders are typically categorized into single-screw and twin-screw types. Twin-screw extruders can be further divided into co-rotating and counter-rotating configurations [12].

Numerous components within the extruder contribute to adjustable process parameters, including the screw configuration, screw speed, feed rate, and temperature profile. Manipulating these parameters allows for the creation of a variety of operating conditions. The screw configuration involves conveying elements that push the reaction mixture forward and kneading elements that generate shear forces for thorough mixing. This intricate interplay of components enables precise control over the REX process, facilitating the achievement of desired outcomes.

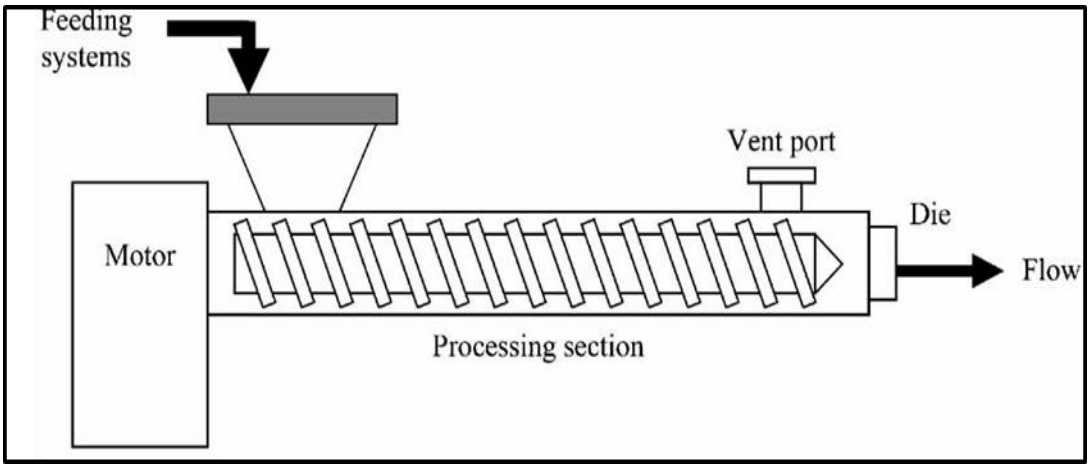

Figure 5: Schematic representation of a reactive extrusion system [12]

Reactive extrusion provides numerous benefits compared to traditional polymer processing methods [13]: It operates as a continuous process, significantly reducing reaction time compared to batch processing. This prevents extended exposure to elevated temperatures that could potentially lead to the undesired thermal degradation of the processed polymer.

a) As a solvent-free process, it eliminates the expenses associated with solvent inlets and recycling systems, while also avoiding the use of potentially harmful solvents, ensuring a safer approach.

b) The shear forces generated by the screw elements spread the reaction mixture, creating thin material layers between the screws. This exposes a substantial surface area available for the reaction to take place. Additionally, this minimizes temperature gradients caused by sudden increases in viscosity during polymerization reactions, ensuring efficient heat and mass transfer within the system.

c) It facilitates effective downstream devolatilization of gaseous byproducts from the reaction mixture, propelling the reaction forward and resulting in heightened efficiency. Its modular construction permits control over multiple processing parameters.

This, combined with the capability to incorporate various input streams, renders REX suitable for a wide spectrum of applications.

Reactive extrusion has found extensive application in the polymerization and modification of numerous biobased and biodegradable plastics. This technique will be the preferred processing method throughout this endeavor [14].

TWIN SCREW EXTRUSION OF HIGH MOLECULAR WEIGHT STEREO-COMPLEX PLA

2.1 Introduction and Background

Research indicates that the role of stereochemistry in determining the material properties of polylactide (PLA) is noteworthy. An increase in the meso-content or D-content during copolymerization with L-lactide leads to a decrease in the polymer's melting point and crystallinity. However, this phenomenon is not observed when physically blending PLLA and PDLA, in contrast to the results from copolymerizing L-lactide and D-lactide. When the interaction between polymers with varying configurations and/or tacticity becomes more influential than the interaction between polymers with similar configurations and/or tacticity, a selective interaction between the polymers emerges. This interaction is known as stereo-complexation [15],

Stereo-complexation in PLA can manifest during polymerization, within solutions, or in the molten state. Drawing from multiple investigations, researchers have inferred that the ratio between stereo-complex crystallites and homo-crystallites is primarily influenced by factors such as the molecular weights and optical purities of the homopolymers, alongside the mixing ratio [16][17]. Through the blending of PLLA and PDLA above their respective melting points, it becomes feasible to create a stereo-complex with a melting point exceeding that of the PLA homopolymers by 50°C. The mechanism underlying the observed elevation in melting temperature is tied to the arrangement of stereo-complex helices, which attain stability through robust van der Waals interactions [18]. **Figure 6** portrays PLA materials with varying tacticity's and configurations, sequenced by ascending melting temperature and crystallinity. While there have been many studies regarding the production of stereo-complex PLA.

The Biobased Materials Research Group (BMRG) has introduced and published a new approach for the extensive manufacturing of this material using a co-rotating twin-screw extruder [19]. Within this section, we will explore the necessary parameters for the high-volume fabrication of stereo-complex PLA within an extruder setup. Additionally, we will delve into the extent of stereo-complex crystallite generation in contrast to the formation of PLA homo-crystallites and its impact as an additive filler for improving the PLA properties.

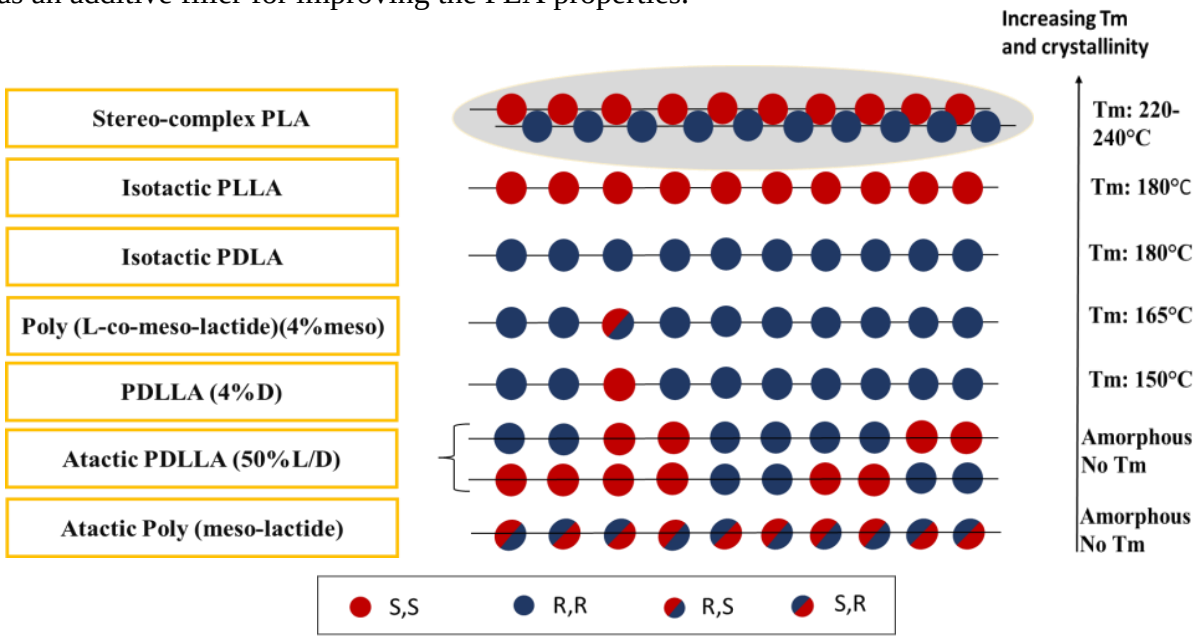

Figure 6: PLA materials of varying configuration and tacticity

2.2 Experimental

2.2.1 Pilot-Scale Manufacturing of Stereo-complex PLA

Materials:

99.99% pure PLLA (L130 and L175) and PDLA (D120) were sourced as pellet forms from Total Corbion and subjected to 24-hour drying at 45ºC. The thermal characteristics, melt flow index (MFI) and relative viscosity (RV) of the employed PLA homopolymers are presented in **Table 1** below.

Subsequently, PLLA and PDLA were combined in specific proportions as mentioned in subsequent sections within an aluminum tray and subjected to an additional 24-hour drying period. Notably, this process did not involve the use of any catalyst or solvent.

Table 1: Material Properties of PLLA and PDLA

Material	D-content	M_w (g/mol)	M_n(g/mol)	MFI(g/10min)	RV (Pa-s)
D120	>99%	106	51	16	2.32
L130	<1%	140	61	16	2.42
L175	<1%	174	82	8	2.73

Twin Screw Extrusion of Stereo-complex PLA:

The methodology herein revolves around the manufacture of stereo-complex PLA using reactive extrusion. Subsequent investigations will delve into processing stereo-complex PLA alongside other materials within an extruder setup. Different combinations of PLLA and PDLA pre-mixtures were introduced into the feeding zone of a co-rotating twin-screw extruder, specifically the ZSE 27 HP–PH model from Leistritz located in Nürnberg, Germany. The screws employed possessed a diameter of 27 mm and an L/D ratio of roughly 40/1, with interchangeable screw elements enabling optimization for various material requirements. The heating system was segmented into 10 distinct heating zones. The dry feed rate was maintained at a constant 3.7 kg/hr, while the screw speed was upheld at 40 rpm. The final shape of the melted product was influenced by the strand die utilized, ultimately resulting in the production of a 3 mm filament. Following quenching in a cold-water bath, the filament underwent pelletization and was subsequently placed within a tray for 24 hours of drying at a temperature of 45ºC. In the creation of complete stereo-complex PLA, it was evident that the screw configuration significantly influenced the extent to which stereo-complex was generated within the extruder. The screw configuration incorporated conveying and

kneading components, responsible for both shear mixing and the necessary duration for the optimal melt blending of PLLA and PDLA, leading to the formation of the stereo complex. Furthermore, left-handed elements were introduced to establish a melt seal, elevating pressure towards the screw's end and thereby extending residence time. The configuration of the screw used for stereo-complex PLA production is illustrated in **Figure 7**.

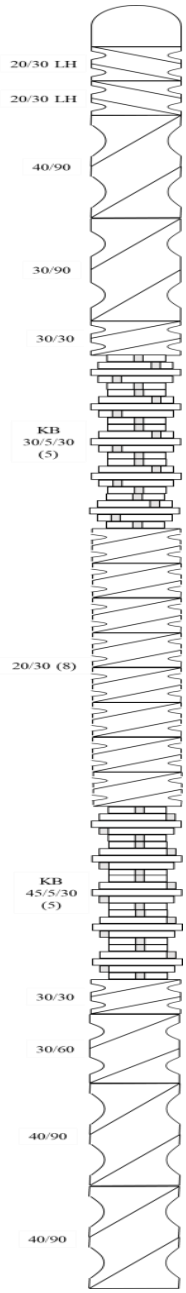

Figure 7: Screw configuration for reactive extrusion of Stereo-complex PLA

In conjunction with the screw configuration, adjustments to the temperature profile were necessary to achieve a uniform melt of stereo-complex PLA. While processing pure PLA alone in an extruder, the primary heating zones are typically set around 10-20ºC above the polymer's melting point (~170-180ºC). However, when blending PLLA and PDLA in different proportions, the evolving stereo-complex within the extruder necessitates a different approach; the melting point notably rises to 220-230ºC. Consequently, certain heating zones towards the extruder's end must be calibrated to align with the melting point of the stereo complex. Otherwise, the product could clog the extruder due to the melt solidifying. This temperature profile ensures thorough mixing of pure PLLA and PDLA melts, while facilitating the passage of the formed stereo-complex PLA through the extruder.

Characterization & Analysis:

Fourier Transform Infrared Spectroscopy (FTIR) was performed using a Shimadzu IRAffinity-1 from 500 to 4600 cm-1 to observe if there were any structural changes in the spectrum of stereo-complex PLA as opposed to neat PLLA.

The decomposition temperature and percentage weight loss were quantified using a thermogravimetric analyzer (TGA), specifically the TGA Q50. About 10 mg of sample was heated from 25 to 550°C at 20 ºC/min.

To verify if and how much stereo-complex PLA was formed, differential scanning calorimetry (DSC) was done with a DSC Q20 on the final product. Two procedures were followed. In the first procedure, temperature was equilibrated to 0 ºC, then ramped up to 260 ºC at a heating rate of 10 ºC/min; temperature was held isothermally for 5 minutes. Afterwards, it was cooled back to 0 ºC at a rate of 10 ºC/min, then held isothermally for 2 minutes.

Finally, the material was heated back to 260 ºC at 10 ºC/min. The second procedure includes a single heating scan procedure whereby temperature was equilibrated to 0 ºC, then ramped up to 260 ºC at a heating rate of 10 ºC/min.

2.2.2 Molecular Composites of Stereo-complex PLA and PLLA

Materials:

3100HP semi-crystalline grade of PLA by NatureWorks, was used as the polymer matrix for composites manufacturing. The material property of the PLA grade is listed below in **Table 2**. Stereo-complex PLA, manufactured in previous section, was utilized as the filler for composites manufacturing through double compounding in the extruder and injection molding.

Table 2: 3100 HP material properties

Sample	α_{obs}^{25} (°)	**o.p. (%)**	**D-content (%)**	M_{wt}% (%)	**Tg (^{o}C)**	**Tpm (^{o}C)**	X_c (%)	**Mn (g/mol)**	**Mw (g/mol)**	**PDI**
3100HP	-154.5	99.04	0.5	1	63.29	176.59	50.14	87	157	1.80

Twin Screw Extrusion and Injection Molding of PLA/Stereo-complex PLA Composites:

PLA/stereo-complex PLA composites were fabricated through two distinct methodologies. The first involved double compounding within a twin-screw extruder, while the second method entailed direct feeding via premixing onto the single hopper in the injection molding machine. The double compounding process was carried out in a pilot-scale co-rotating twin-screw extruder, characterized by an L/D ratio of 48 and a screw diameter of 26 mm.

For the direct premix approach, an 85-ton Cincinnati Milacron injection molding machine from Ohio, USA, was utilized. Four distinct compositions (8%, 9%, 12%, and 18%) were investigated to assess the influence of stereo-complex PLA, aiming to examine its potential as an additive filler to enhance mechanical properties. For smaller stereo-complex PLA proportions, direct pre-mixing into the injection molding machine was employed.

While for higher proportions, the stereo- complex PLA underwent melt blending within the twin-screw extruder through double compounding. Subsequently, a comparative analysis was conducted between the double- compounded melt blend and the batch pre-mix directly introduced into the injection molding machine for higher letdowns.

PLA homopolymer matrix, in the form of pellets, was first pre-mixed with stereo-complex PLA filler, also in the form of pellets. The mixtures were then dried for 48 hours at 50°C. The temperature profile used on the extruder from the feed section to the die was as follows: 160/170/180/190/190/190/195/195/195/190/190. This temperature profile was chosen to allow for viscous flow of the PLA matrix (melting peak temperature T_{pm} = 180°C for 3100HP) while allowing for dispersion of the stereo-complex PLA filler without melting. This is also to prevent thermal dissociation of the stereo-complex PLA filler.

A feed rate of 4 kg/hour and screw speed of 100 rpm was chosen. The screw configuration was constructed to allow for optimal mixing and transport of the PLA homopolymer matrix and stereo-complex PLA filler. Kneading elements were placed in the first and second half of the barrel in between the conveying elements.

This was to allow for mixing in the first and last minute of processing, while enabling material transport throughout the extruder. Residence time was 4 minutes until the product was extruded out of a 5 mm diameter strand die, then quenched in a cold-water bath and pelletized. Samples were collected at different time intervals to account for the dispersity of the filler in the matrix. Samples were then dried in an oven at 55°C for 24 hours, then characterized.

Characterization and Analysis:

DSC was conducted using a TA Instruments DSC Q20 to characterize the dispersity of stereo-complex PLA filler in PLA homopolymer matrix at different time intervals. The temperature was first equilibrated to 0 ºC, then the temperature was ramped up to 260 ºC at a heating rate of 10 ºC/

min. A second heating scan was not run because, above its melting peak temperature (~238°C), stereo-complex PLA thermally dissociates into its constituent homopolymers.

The tensile test specimens for the molecular composites were prepared using an 85-ton Cincinnati Milacron (Ohio, USA) injection molding machine. The barrel and nozzle temperatures were set at 380/350/350 ºF and 375 ºF respectively. The mold was held at room temperature. The screw speed was set to 100 rpm and the injection pressure used was 800 psi. The total cycle time was set at around ~90s. Thermal annealing of the injection molded test specimens was performed using a regular lab-scale convection oven. The oven was heated to 100 ºC before introducing the samples, which were placed in an aluminum tray. Samples were placed in a manner to minimize warpage during the annealing process.

The tensile testing was carried out on an Instron model 5565-P6021 (Massachusetts, USA) mechanical testing fixture setup with a 5 kN load cell. The testing was carried out in accordance with the ASTM D638-14 (Type I sample size) standard test method for tensile properties of plastics [8]. The rate of grip separation was set at 5 mm/min which was as per the ASTM D638 specifications. A minimum of five replicates were used to ensure repeatability of the test data.

The notched Izod impact properties were studied using a Ray-Ran RR-IMT (Warwickshire, UK) pendulum impact tester equipped with a Techni-Test test software. The testing was carried out in accordance with the ASTM D256 standard test method for determining the Izod pendulum impact resistance of plastics [9]. The samples were notched using a Tinius Olsen Model 22-05-03 Motorized Specimen Notcher (Pennsylvania, USA).

The test specimens had dimensions of 63.5 mm X 12.7 mm and the notch marked was 2.54 mm deep. A minimum of five replicates were used to ensure repeatability of the test data.

2.3 Results and Discussion

Numerous research endeavors have been conducted to explore the production of stereo-complex PLA utilizing a range of additives, nucleating agents, rheometers, and solvent-based techniques [20][21][22][23]. **Table 3** provides a comprehensive overview of the findings in contrast to our methodology. Gupta et al. conducted a comparable solution casting approach employing varying compositions (1-3wt%) of modified chitosan (MCH). While they achieved stereo-complexation exceeding 99.99%, this outcome was observed at the highest additive concentration (3% MCH). Notably, the melting peak temperature of the stereo-complex was quite low at approximately 206°C, accompanied by a relatively modest crystallinity level of around 35% as determined through DSC analysis [23]. Su et al. presented an additive-free, solventless technique employing micro-extrusion within a rheometer to synthesize stereo-complex PLA from high molecular weight PLLA and PDLA. This approach achieved stereo-complexation surpassing 99.99%, marked by a melting peak temperature of roughly 230°C and crystallinity reaching approximately 44% [20].

Table 3: Recent Studies on Stereo-complex PLA

Group	**Method**	***fsc* (%)**	**Tpm,sc (°C)**	***Xsc* (%)**
Xie [21]	Solution casting with BTCA	60	220	23
Gupta [23]	Solution casting with MCH	100	206	35
Su [20]	Rheometer (190-220°C)	100	230	44
Korber [22]	Co-rotating twin screw extrusion (180-240°C)	25	220	10
BMRG [19]	Co-rotating twin screw extrusion (180-220°C)	95	240	58

To upscale this process, Korber et al. applied a pilot-scale co-rotating twin-screw extruder [22]. Without additives/nucleators, only ~25% stereo-complex formation occurred, with a stereo-complex melting peak temperature of ~220°C.

BMRG has published an article that provides a clear scalable, solventless, additive-free technique to produce exclusive stereo-complex [19]. in the extruder. **Figure 8** depicts the formation of stereo-complex PLA in an extruder using a structural sketch of the polymer chains.

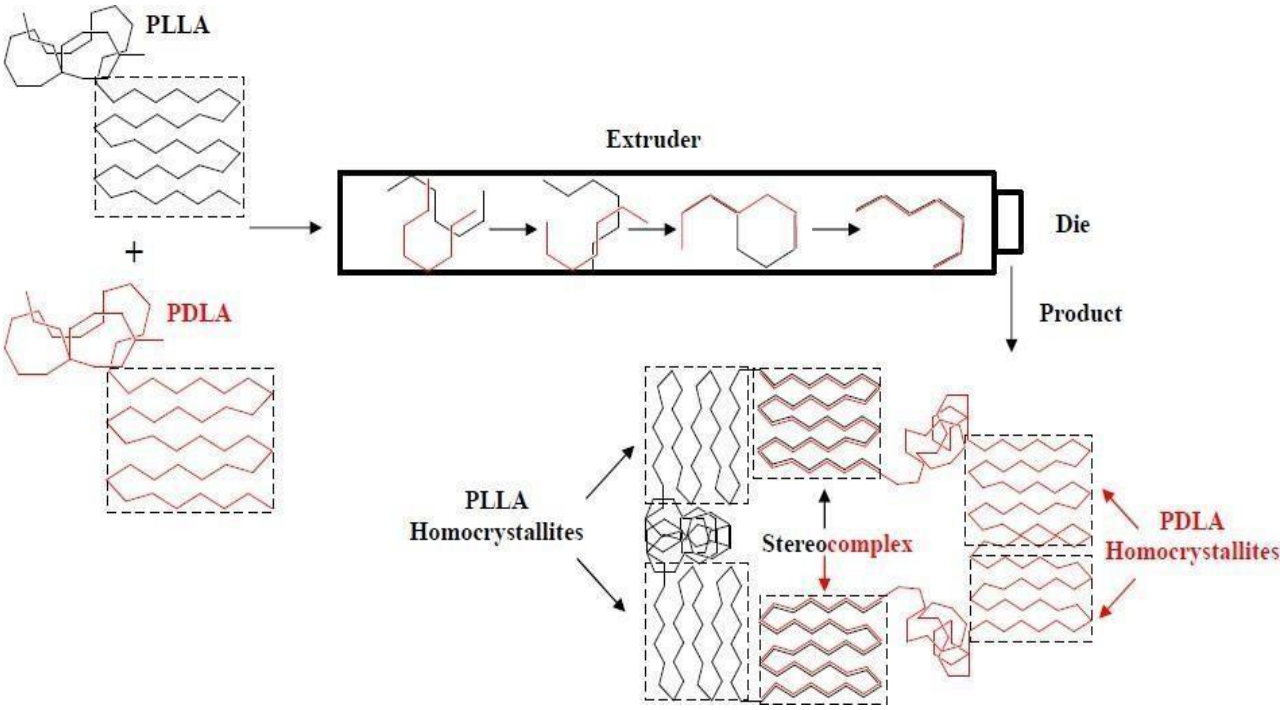

Figure 8: Schematic Representation of competitive formation of Stereo-complex crystallites

2.3.1 Pilot-Scale Manufacturing of Stereo-complex PLA

Characteristics of Stereo-complex Formation:

The characteristics related to the creation of stereo-complexes through reactive extrusion are primarily controlled by temperature. Other factors like screw design, length-to-diameter ratio (L/D), and throughput are closely intertwined, especially in terms of process scalability and continuity. In the context of a particular setup and design parameters in a co-rotating twin-screw extruder, achieving a specific mechanical output is crucial for a successful transition of the process. Stereo-complex formation happens almost instantly when operating at temperatures higher than the melting point of pure PLA polymer. Earlier, attempts to optimize temperature were done in 10°C intervals between 180°C and 230°C.

The results indicated a direct relationship between the percentage of stereo-complexation and temperature, which tapered off as the stereo-complex PLA approached its highest melting point. Beyond this melting point, the outcomes demonstrated a thermal dissociation phenomenon into the individual homo-polymeric components, PLLA and PDLA. This can be attributed to the increased chain mobility within PLLA and PDLA. As temperature approaches the highest melting point, molecular movement rises, leading to higher entropy. The research emphasizes that while temperature significantly influences the stereo-complexation process, the role of time is comparatively less important.

Confirmation of Stereo-complex Formation via ATR-FTIR:

Formation of stereo-complex PLA was confirmed via FTIR spectra (**Figure 9**). The spectrum in **Figure 9a** shows that there is no significant structural change in the spectrum compared to PLLA. However, stereo-complex formation can be characterized by the absorption band at 908 cm-1, as seen in **Figure 9b** [24].

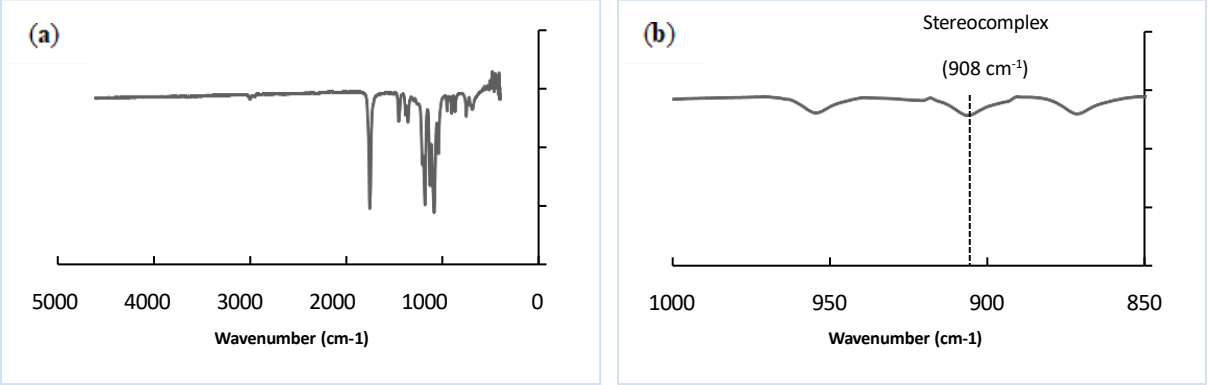

Figure 9:(a) FTIR spectra of Stereo-complex PLA (b) Characteristic absorption bands of Stereo-complex PLA

Thermal Degradation of Stereo-complex PLA:

Using TGA analysis, the thermal decomposition temperature of stereo-complex PLA was determined and compared to synthesized poly(L-lactide). As seen in (**Figure 10a**), the decomposition temperature of stereo-complex PLA was analyzed to be ~376°C, with a percent weight loss of ~98%; the polymer starts to decompose at ~296°C. This is higher than our synthesized PLLA (**Figure 10b**), whose decomposition temperature was determined to be ~361°C with a percent weight loss of ~96%; the polymer starts to decompose at ~243°C.

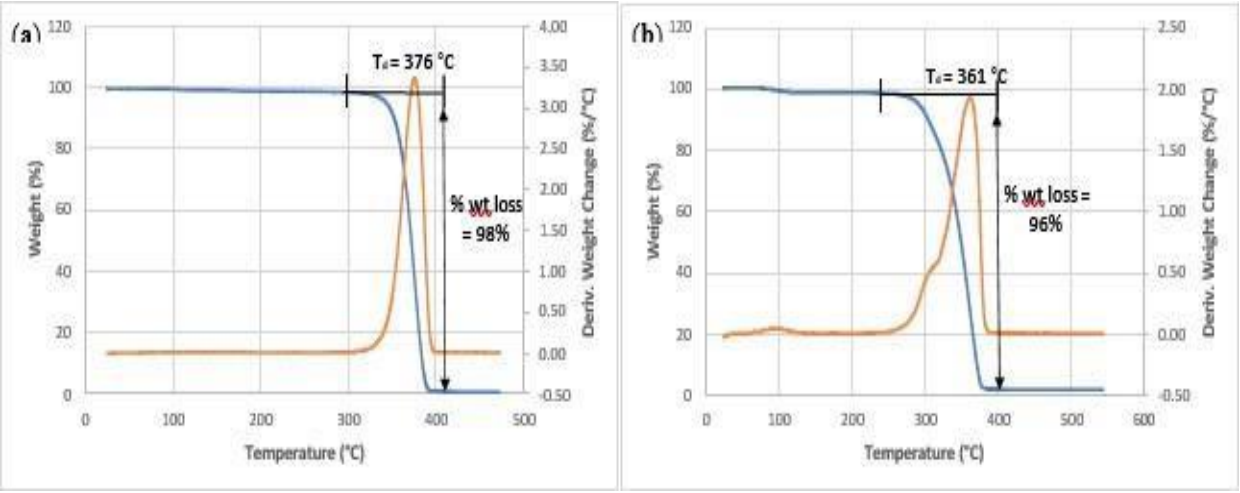

Figure 10: Thermal stability of (a) Stereo-complex PLA and (b) Poly(L-lactide)

This difference in the decomposition temperature may be attributed to the stabilizing van der Waals interactions that are formed between opposite hydrogen and oxygen atoms in stereo-complex PLA. These powerful interactions in the complex stabilize the 31-helix and thus cause the higher decomposition temperature and melting point in stereo-complex PLA.

Thermal Characterization of Stereo-complex PLA:

DSC analysis was employed to validate the crystalline nature of PLA concerning varying ratios of PDLA. The first heating scan using DSC (**Figure 11**) depicted the formation of stereo-complex PLA through different initial mix ratios of PDLA. Various compositions of PDLA (D120) ranging from 25% to 50% were combined with PLLA (L130).

The processing conditions involving twin-screw extrusion, including temperature profile, screw speed, and configuration, were kept constant to assess how different ratios affected the percentage of stereo-complexation. As the PDLA content percentage increased, the enthalpy associated with the individual homo-polymers notably decreased. At a 50% PDLA content, the majority of crystallinity originated from stereo-complex crystallites, accounting for approximately 97%. A comparative overview of glass transition temperature, melting point, and percent crystallinity can be found in **Table 4**.

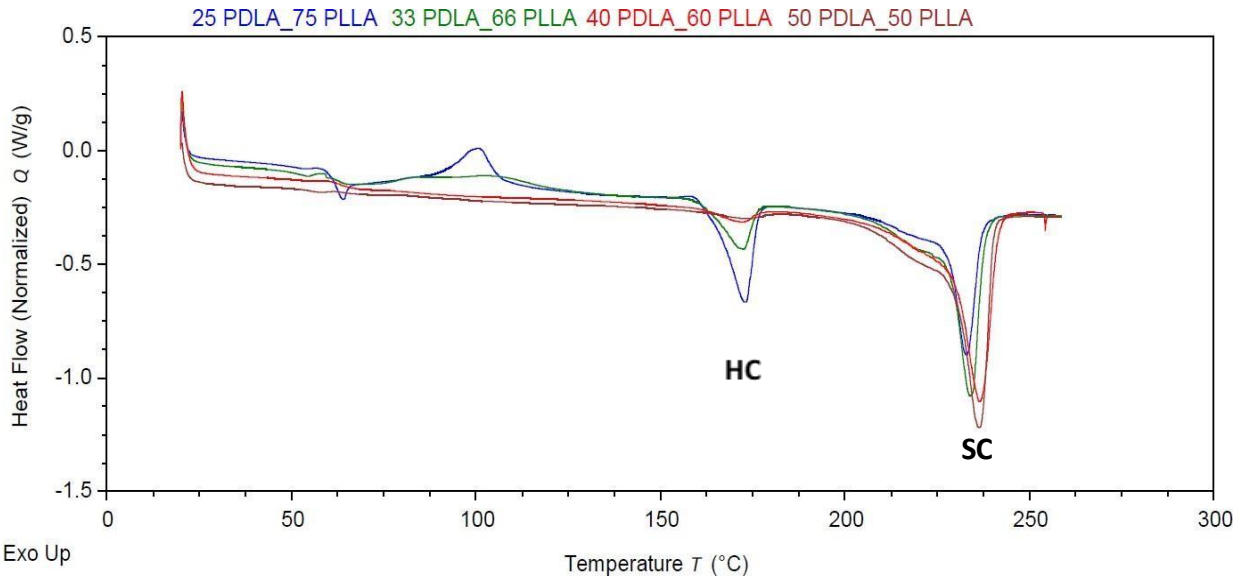

Figure 11: Stereo-complexation varying PDLA content

Table 4: Comparative Table for thermal properties of different %PDLA run.

Run	Tg (°C)	ΔHm (J/g) (HC)	%Crystallinity (HC)	ΔHm (J/g) (SC)	%Crystallinity (SC)	Total Crystallinity
25% PDLA	60.17	22.4	7.5	47.6	**33.3**	40.8
33% PDLA	59.53	11.1	11.9	51.3	**35.8**	47.7
40% PDLA	59.7	3	3.2	55.6	**38.8**	42
50% PDLA	59.6	1.6	1.7	77.2	**54**	55.6

2.3.2 Molecular Composites of Stereo-complex PLA and PLLA

Thermal Characterization of PLA/Stereo-complex PLA Composites:

Based on the results from different PDLA input run, two different compositions comprising of 25% PDLA + 75% PLLA (MB1) and 50% PDLA +50% PLLA (MB2) were carried forward for making PLLA based composites. The following figure shows the first DSC heating scan of MB1 and MB2 at different time intervals collected while bulk processing in the twin screw extruder.

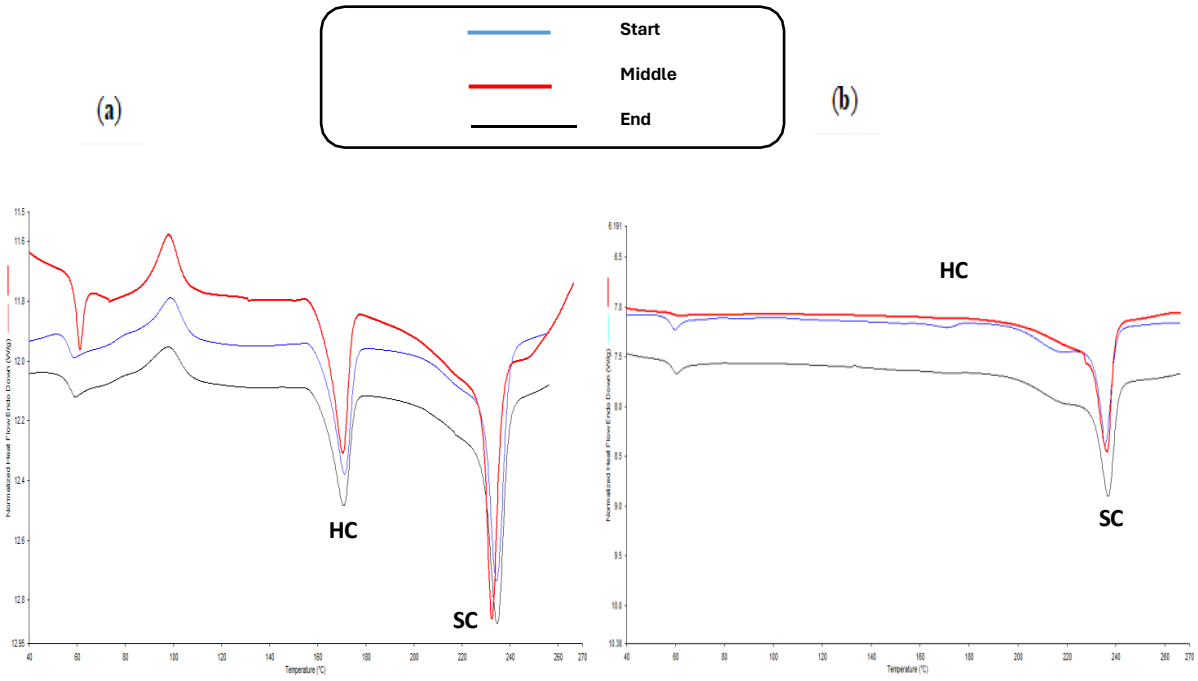

Figure 12: First DSC heating Scan of (a) MB1 and (b) MB2

The below **Table 5** summarizes the % stereo-complex crystallinity observed while processing the two different PDLA ratios. The findings indicate that processing a blend of 25% PDLA and 75% PLLA through the twin-screw leads to an average stereo-complex (SC) crystallinity of approximately 33.8%. Similarly, when using a blend of 50% PDLA and 50% PLLA, the SC crystallinity reaches about 56.7%.

Table 5: Thermal properties of sample at different time intervals for (a) MB1 and (b) MB2

Sample Name	ΔH (HC) (J/g)	%χ (HC)	ΔH (SC) (J/g)	%χ (SC)	Total χ
MB1 (Start)	11.9	12.7	47.6	**33.3**	46
MB1 (Middle)	14.7	15.7	48.3	**33.8**	49.5
MB1 (End)	13.3	14.2	49.4	**34.5**	48.7
Average and SD				**33.8 ± 0.603**	48.07 ± 1.83

Sample Name	ΔH (HC) (J/g)	%χ (HC)	ΔH (SC) (J/g)	%χ (SC)	Total χ
MB1 (Start)	11.9	12.7	47.6	**33.3**	46
MB1 (Middle)	14.7	15.7	48.3	**33.8**	49.5
MB1 (End)	13.3	14.2	49.4	**34.5**	48.7
Average and SD				**33.8 ± 0.603**	48.07 ± 1.83

After processing the samples labeled as MB1 and MB2, they underwent double compounding in a twin-screw extruder with 3100 HP, at higher letdown percentages of 36.1% and 33.7%, respectively. Predicted SC crystallinity in the composite sample was calculated based on the letdown percentage. These double compound pellets were subsequently introduced into an injection molding machine utilizing single screw conveying and a temperature profile ranging from 180 ºC to 195 ºC. Notably, no additional stereo-complexation was observed during the

secondary process of crafting the dumbbell-shaped test bars. **Figure 13** showcases the first DSC heating scan of the composite samples with 3100 HP, offering valuable alignment between experimental SC crystallinity and actual results.

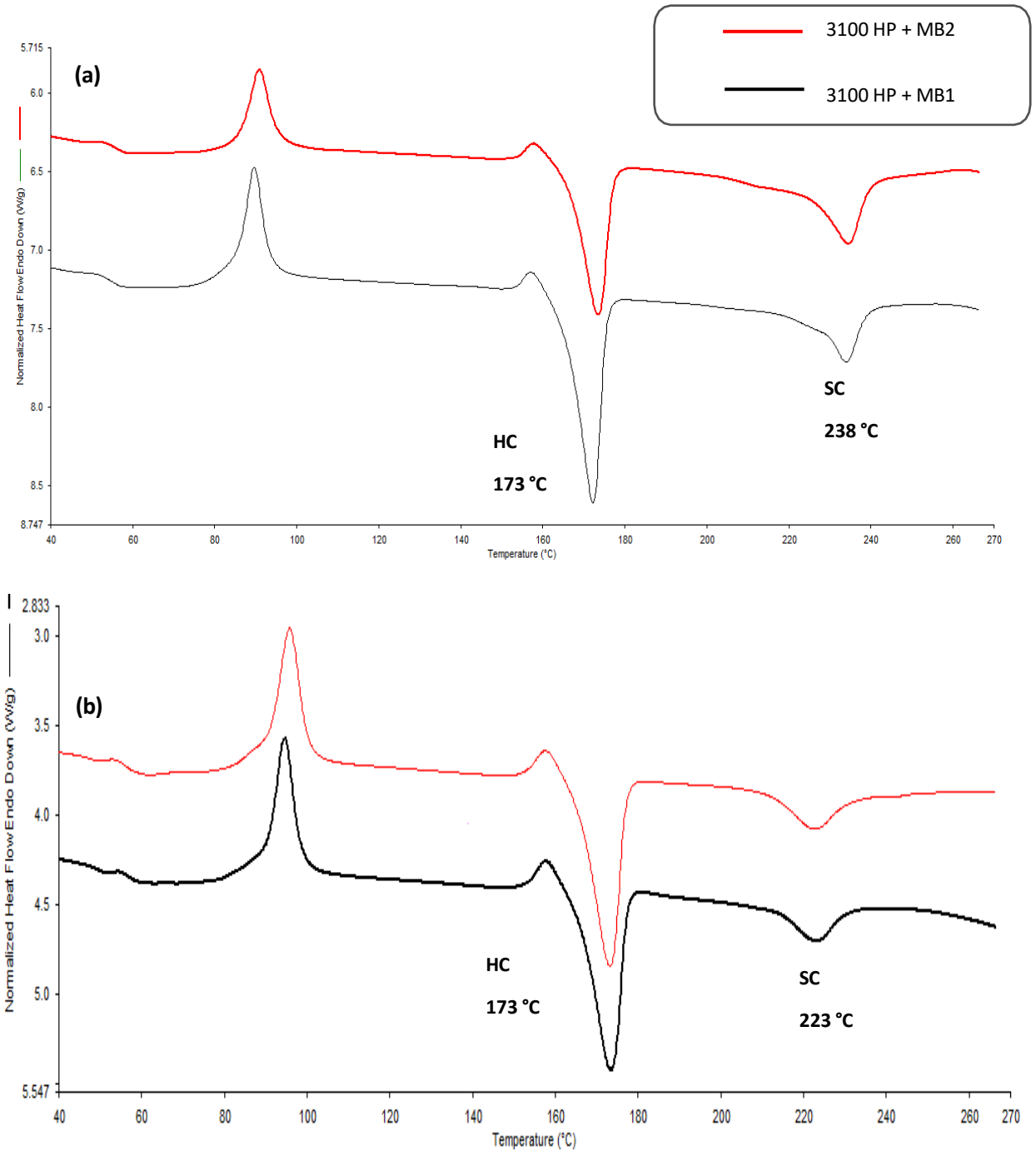

Figure 13: First DSC scan of PLA composites (a) Double Compounding (b) IM

Table 6: Thermal Properties of the PLA composites

Sample Name	Masterbatch letdown	Expected SC crystallinity	% D content	ΔH (SC)	%χ (SC)
Double Compounding					
3100 HP + MB1	36.1 %	**12.2**	9%	22.7	**12.4**
3100 HP + MB2	33.7%	**19.1**	16.9%	29.1	**20.3**

Sample Name	Masterbatch letdown	Expected SC crystallinity	% D content	ΔH (SC)	%χ (SC)
Direct Premix (IM)					
3100 HP + MB1	36.1 %	**12.2**	9%	12.4	**8.6**
3100 HP + MB2	25.4 %	**14.4**	12.7%	11.5	**8.0**

When directly premixing into the injection molding machine, a notable observation was made. Maintaining a barrel temperature profile like the melt temperatures during the second twin-screw extrusion resulted in test bars exhibiting white specks. This indicates that the single-screw extruder within the injection molding machine is not as effective in achieving distributive mixing compared to the twin-screw extruder. The temperatures were elevated beyond the peak melting temperature of the stereo-complex PLA.

Consequently, a reduction in the peak melting temperature of the stereo-complex PLA was observed. Furthermore, the extent of stereo-complexation was diminished, reaching an equilibrium at approximately 8%. This equilibrium can be attributed to the presence of PDLA to a certain degree within the composition.

Mechanical Properties of PLA/Stereo-complex PLA Composites:

Tensile Testing and Impact Testing was done on Neat 3100 HP and the composites formulated through double compounding and direct premix. With MB1 double compounding and having % stereo-complex 12.4 % we see 16.25% increase in the tensile stress and impact strength at break compared to Neat 3100 HP. It is evident that % Stx crystallinity in the sample depends on the right process selection and that has an influence on the mechanical properties.

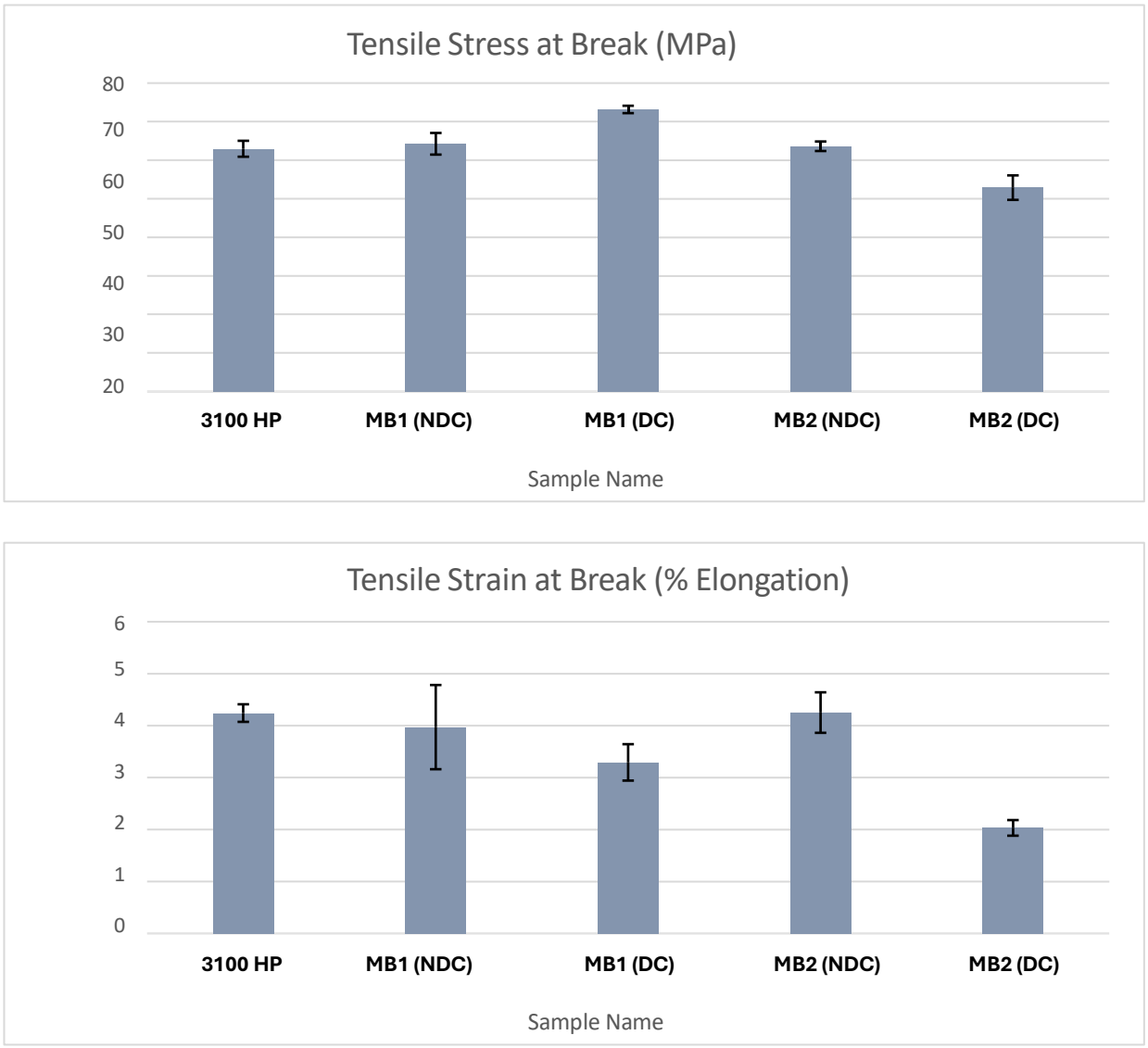

Figure 14: Tensile Properties of Neat 3100 HP and Stx-Composites

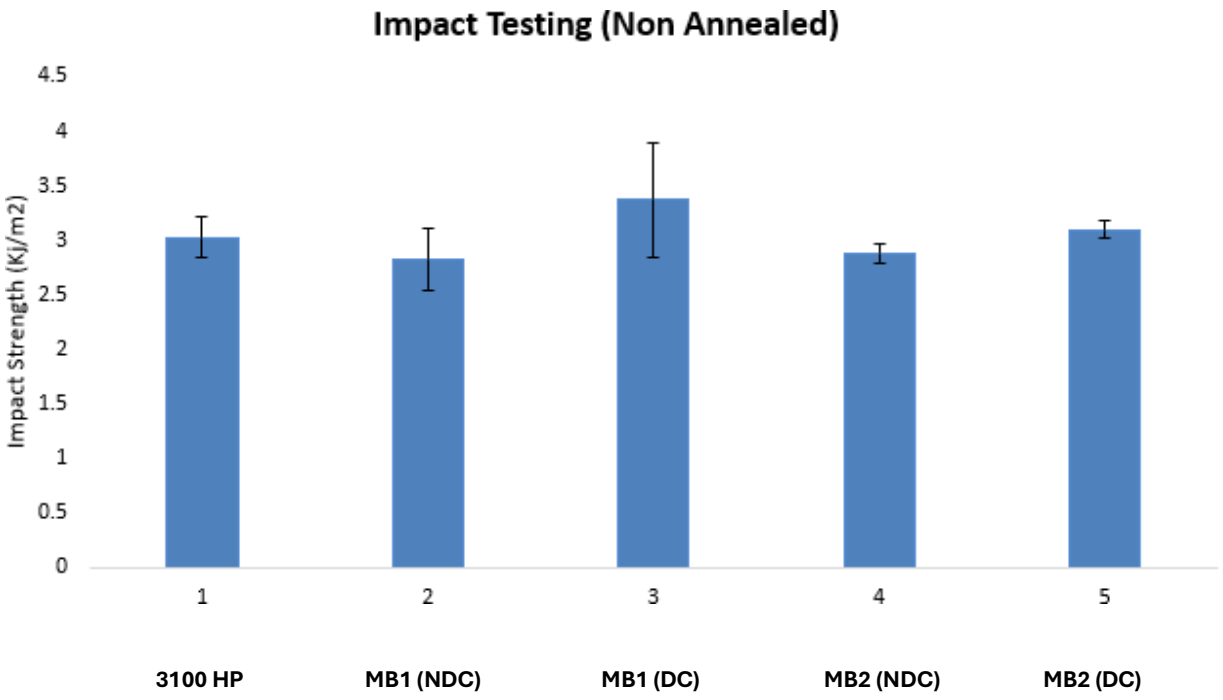

Figure 15: Impact Properties of Neat 3100 HP and Stx-Composites

2.4 Conclusion and Next Steps

As DSC and FTIR have confirmed, we have successfully produced >95% stereo-complex PLA. This was depicted by its high melting point, which is attributed to the strong van der Waals interactions, formed between opposite hydrogen and oxygen atoms, that stabilize the helices associated with PLA. While stereo-complex PLA was formed, it is important to note that heating it above its melting point will dissociate the stereo-complex PLA back to the original PLA homopolymers used to produce the final material. However, if the material is heated below its melting point, the stereo-complex will be maintained, and no dissociation will occur. Next steps involve utilizing stereo-complex PLA at lower letdowns as nucleating agent. Alternate grade of PLA for further understanding the influence of molecular composites and exploring applications in films.

BIOBASED COMPOSTABLE COATINGS FOR PAPER COATING APPLICATION

3.1 Introduction and Background

The principles of sustainable development and eco-design are pivotal across various domains. Eco-design involves a product design approach that prioritizes the environmental impact throughout its entire lifecycle. This concept has gained substantial traction in packaging design, with the primary aim of packaging being to safeguard items from production to usage. This entails optimizing material, water, and energy usage, while also minimizing waste and enhancing the recovery of used packaging [25]. Adopting sustainable packaging design principles, which include effectiveness, efficiency, cyclicality, and safety, is crucial in this endeavor [26].

For packaging with shorter lifespans, material choice becomes even more vital. The preference shifts toward using materials sourced from renewable origins, which are recyclable or compostable. Designing for maximum sustainability and recoverability is essential in these cases. Protective paper packaging serves a multitude of purposes, such as product transportation, storage protection, and filling space within boxes [27]. Paper, a widely used packaging material, holds the advantage of being biodegradable and environmentally friendly. However, efforts to enhance barrier resistance and wettability often entail the application of petroleum-based derivatives like polyethylene, waxes, or fluor-derivatives as coatings, leading to compromised biodegradation and recyclability [28][29].

Petroleum-based polymers, due to their limited recyclability and non-biodegradability, constitute a massive portion of global waste. A more sustainable option involves using naturally renewable biopolymers as barrier coatings on paper packaging materials. Polylactide (PLA), a promising polymer, stands out due to its biocompatibility, biodegradability, and its derivation from bio-based sources. PLA is versatile, suitable for processes like injection molding, extrusion, foaming, thermoforming, and various coating techniques [26].

This chapter of the research is divided into two primary sections. Firstly, it focuses on the synthesis and unique characteristics of Poly(meso-lactide) (PML), exploring its application in paper coating. The second part revolves around the modification of commercially available PLA using organo-silane functionality through reactive extrusion (REX). Additionally, it entails coating the commercial grade PLA's including Poly (meso-lactide) (PML) and modified PLA onto Kraft paper via roll coating to assess its suitability for paper coating applications.

3.2 Experimental

3.2.1 Melt Polymerization of Meso-lactide

Materials:

Meso-lactide (M700) was purchased from NatureWorks. It was recrystallized twice using ethyl acetate, and once using anhydrous toluene. It was vacuum dried at 35ºC for 48 hours, then stored in an argon atmosphere at -20 ºC. Using NMR and DSC, 99.7% monomer purity was determined for meso-lactide. Stannous octoate was the main catalyst used for polymerization of meso-lactide and was purchased from Millipore Sigma. Triphenyl Phosphine was used along with the catalyst and was purchased from Millipore Sigma. Deuterated chloroform (CDCl3), HPLC grade chloroform (CHCl3), HPLC grade tetrahydrofuran (THF), and anhydrous toluene were also purchased from Millipore Sigma. HPLC grade dichloromethane (DCM) and ethyl acetate were both obtained directly from VWR. These reagents were used as is and not purified any further.

Characteristics of Poly(meso-lactide):

Poly(meso-lactide) was synthesized using Natureworks' M700 standard grade of pure meso-lactide; 99.7% purity was reported after recrystallization three times with anhydrous toluene.

The reaction vessel and other glassware components were dried in an oven at 120 ºC for 24 hours. The vessel was then flame-dried and purged with Argon before adding the monomer.

Then, the monomer and vessel were vacuum dried at 40ºC for 48 hours. Synthesis occurred for 2&1/2 hours under rigorous mixing at 120 RPM, at a constant melting temperature of 180 ºC; Stannous Octoate (M/C=5000) was the main catalyst used in the reaction. An equimolar ratio of Triphenyl Phosphine (P(Ph)3) was added along with the catalyst. The reaction is based on a coordination insertion mechanism, where a hydroxyl compound is required as an initiator. The alcohol first reacts with the catalyst to form a tin alkoxide bond by ligand exchange. Afterwards, stannous octoate's tin atom coordinates with an exocyclic carbonyl oxygen from lactide in the alkoxide form; this coordination enhances the lactide carbonyl group's electrophilicity and initiator's alkoxide group nucleophilicity. The acyl-oxygen bond of the lactide breaks, "opening" the lactide chain to allow insertion into the alkoxide of the catalyst. This is followed by polymer propagation as the lactide molecules are added to the tin-oxygen bond, forming the polymer [30][31]. For transfer purposes, a 4wt% catalyst solution was prepared in anhydrous toluene.

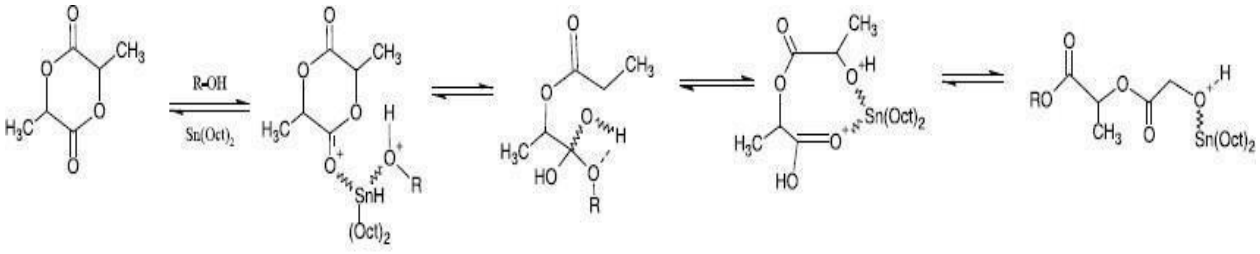

Figure 16: Ring opening polymerization (ROP) of lactide

Characterization & Analysis:

Using a Shimadzu IRAffinity-1, the chemical structure of PLA was verified by FTIR spectra from 500 to 4600 cm-1.

Differential scanning calorimetry (DSC) was done with a DSC Q20 to calculate purity of the monomer and further the thermal properties of the synthesized Poly (meso-lactide). The procedure was as follows. Temperature was equilibrated to 0 ºC, then ramped up to 200 ºC at a heating rate of 10 ºC/min; temperature was held isothermally for 5 minutes. Afterwards, it was cooled back to 0 ºC at a rate of 10 ºC/min, then held isothermally for 2 minutes. Finally, the material was heated back to 200 ºC at 10 ºC/min.

The decomposition temperature and percentage weight loss were quantified using a thermogravimetric analyzer (TGA), specifically the TGA Q50. About 10 mg of sample was heated from 25 to 550 °C at 20 ºC/min.

The tacticity was also confirmed by procuring the H^1 NMR spectrum for the polymer, using an Agilent DDR2 500 MHz NMR spectrometer equipped with 7600AS 96 sample autosamplers running VnmrJ 3.2A.

The spectrum was acquired from ~0.2% solutions in $CDCl_3$, with the methyl protons decoupled from the methine protons during the acquisition time. The monomer conversion was also quantified by H^1 NMR spectroscopy; the methine protons have different chemical shifts in the monomer (5.04 ppm) from the polymer (5.13–5.25 ppm). Integrating the area under each peak will directly provide the percent monomer conversion.

Viscosity is dependent on molecular weight distribution; correlations have been made between dilute solution viscosity and molecular weight. The ASTM D2857-16: Standard Practice for Dilute Solution Viscosity of Polymers and Intrinsic Viscosity of Polymer and Biopolymers Measured by Microchip has been referenced for the following procedure of viscosity and molecular weight determination. A constant-volume viscometer was used inside a fume hood operating at 27°C for all trials. The primary viscometer used was Canon 0C-D290.

For one polymer sample, four trial concentrations were made by adding the required sample weight (mg) to a vial of 15ml of chloroform. The trial concentration in the vial was poured through a funnel into the viscometer. The sample was plunged up into the viscometer with a syringe. Using a stopwatch, the solution's passage through the marked region of the viscometer was timed to obtain an efflux time. This was repeated three times for each sample concentration and pure solvent sample. The average of the sample efflux times was used in viscosity calculations.

3.2.2 Silylation of PLA via REX

Materials:

Poly(meso-lactide) from the previous section was utilized alongside 752-27 and 3100 HP industrial grade of PLA purchased from NatureWorks. Vinyl-trimethoxysilane (VTMOS, bp = 123 °C) and 2,5-Bis(tert-butylperoxy)-2,5-dimethylhexane (Luperox 101) were obtained from Sigma Aldrich (WI, USA). The PLA resin pellets of 752-27 AND 3100 HP were subjected to a 24-hour drying period at 50 ºC.

Silylation Chemistry on PLA:

The process of attaching vinyl-trimethoxy silane (VTMOS) to the PLA backbone is elucidated in Figure 13. This mechanism, involving melt free radical grafting through vinyl functionality, is widely acknowledged and has been effectively employed to introduce various chemical species into PLA [32]. The initial step involves the thermal decomposition of a free radical initiator (Luperox), yielding radicals. These radicals' abstract hydrogen from the α-carbon position, generating radicals on the PLA chain. This hydrogen abstraction from PLA was initially demonstrated by Avella et al. [33] in the reaction with butyl acrylate. Subsequently, the generated PLA radicals can bind with radicals present on the vinyl group of VTMOS.

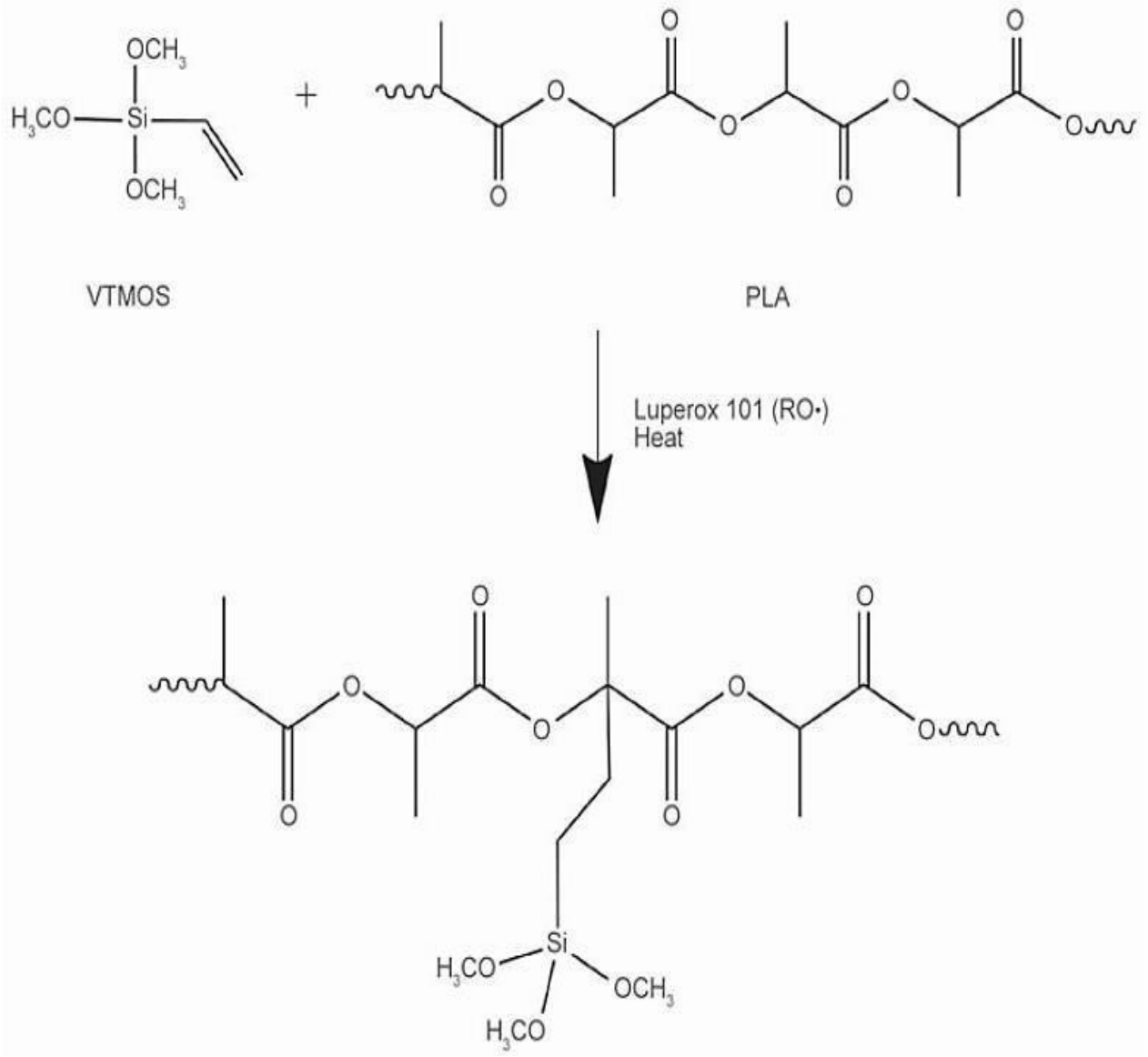

Figure 17: Schematic Representation for free radical initiated grafting of VTMOS on PLA

The silylation for poly(meso-lactide) was carried out in Parr 4848 and for industrial grade PLA it was carried out on co-rotating twin screw extruder 27 HP–PH model from Leistritz located in Nürnberg, Germany. Following temperature profile and screw configuration was adopted for PLA grafting. PLA along with free radical initiator and VTMOS were premixed and fed into the hooper. 1 wt.% of VTMOS and 0.25 wt.% of catalyst was utilized.

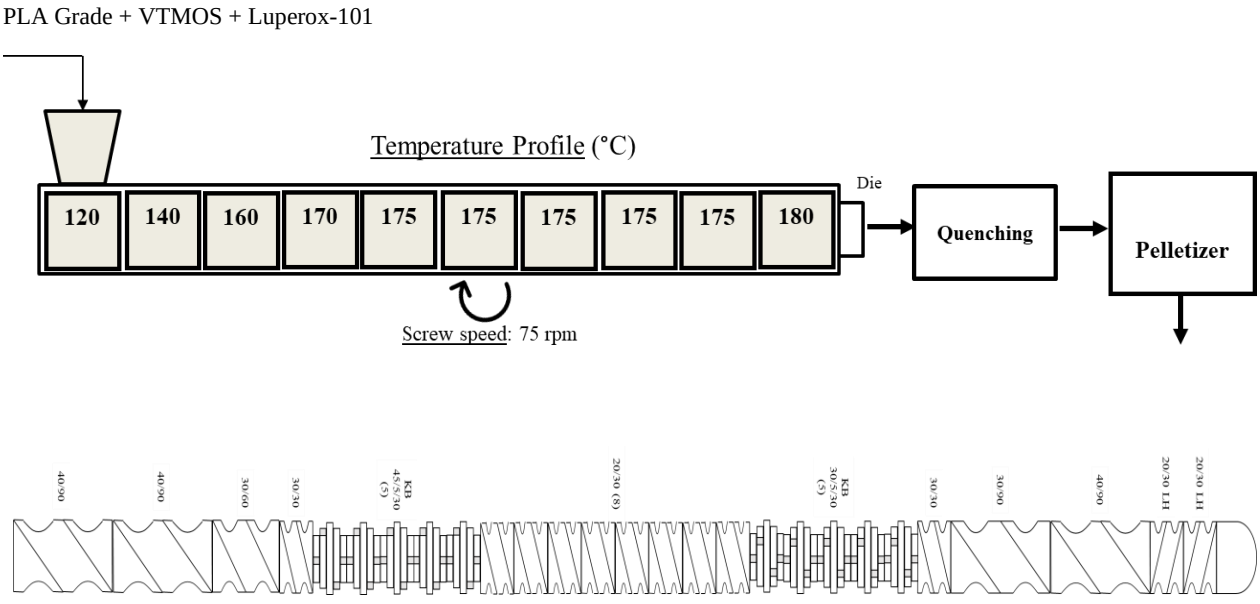

Figure 18: REX for Silylation of PLA

Characterization and Analysis:

Thermal characterization of modified PLA was conducted using a DSC Q20 instrument to assess its thermal behavior. The testing procedure involved initial temperature equilibration at 0 ºC, followed by gradual heating to 200 ºC at a rate of 10 ºC/min. This temperature was maintained isothermally for 5 minutes. Subsequently, the sample was cooled back to 0 ºC at the same rate, and a 2-minute isothermal hold was performed. Finally, the material was reheated to 200 ºC at 10 ºC/min.

The verification of the modified PLA's chemical structure was carried out using a Shimadzu IRAffinity-1 instrument, which acquired FTIR spectra spanning the range of 500 to 4600 cm-1. To confirm the grafting of VTMOS onto PLA, H^1 NMR spectrum was obtained using an Agilent DDR2 500 MHz NMR spectrometer equipped with 7600AS 96-sample autosamplers running VnmrJ 3.2A.

3.3 Results and Discussion

Synthesis of poly(meso-lactide) was confirmed in the below FTIR spectra (**Figure 19**). The spectrum showed peaks corresponding to asymmetric (3035 cm^{-1}) and symmetric –CH stretching (2910 cm^{-1}). The peak at 1757 cm^{-1} confirms polymerization, as lactide's peak is generally at ~1725 cm^{-1}

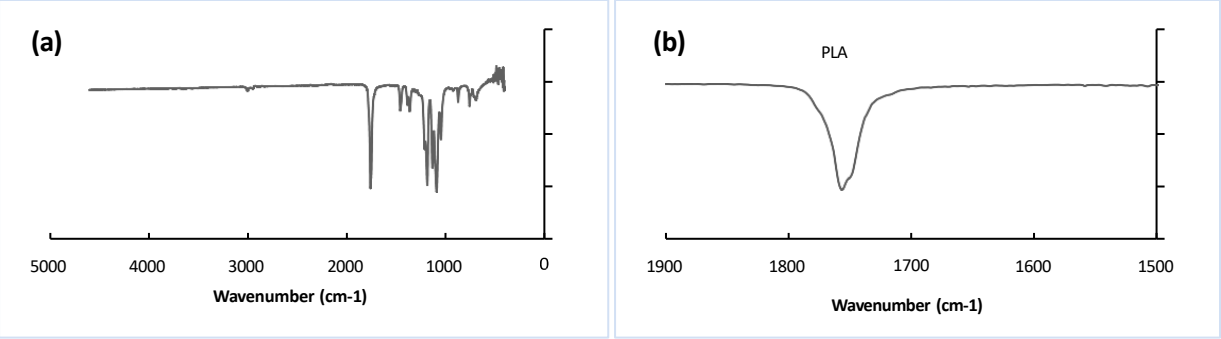

Figure 19: (a) FTIR spectra of poly(meso-lactide) (b) Confirmation of PLA polymerization characterized by the absorption band at ~1725 cm^{-1}

Using TGA analysis, the thermal decomposition temperature of poly(meso-lactide) was determined and compared to synthesized poly(L-lactide). From **Figure 20**, the decomposition temperature was analyzed to be ~324°C, with a percent weight loss of ~96%.

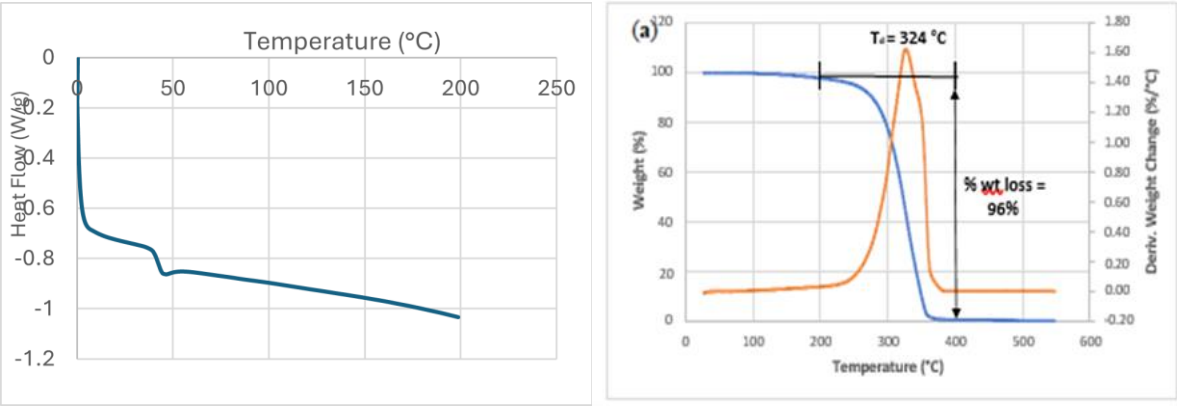

Figure 20: TGA and DSC curves of PML

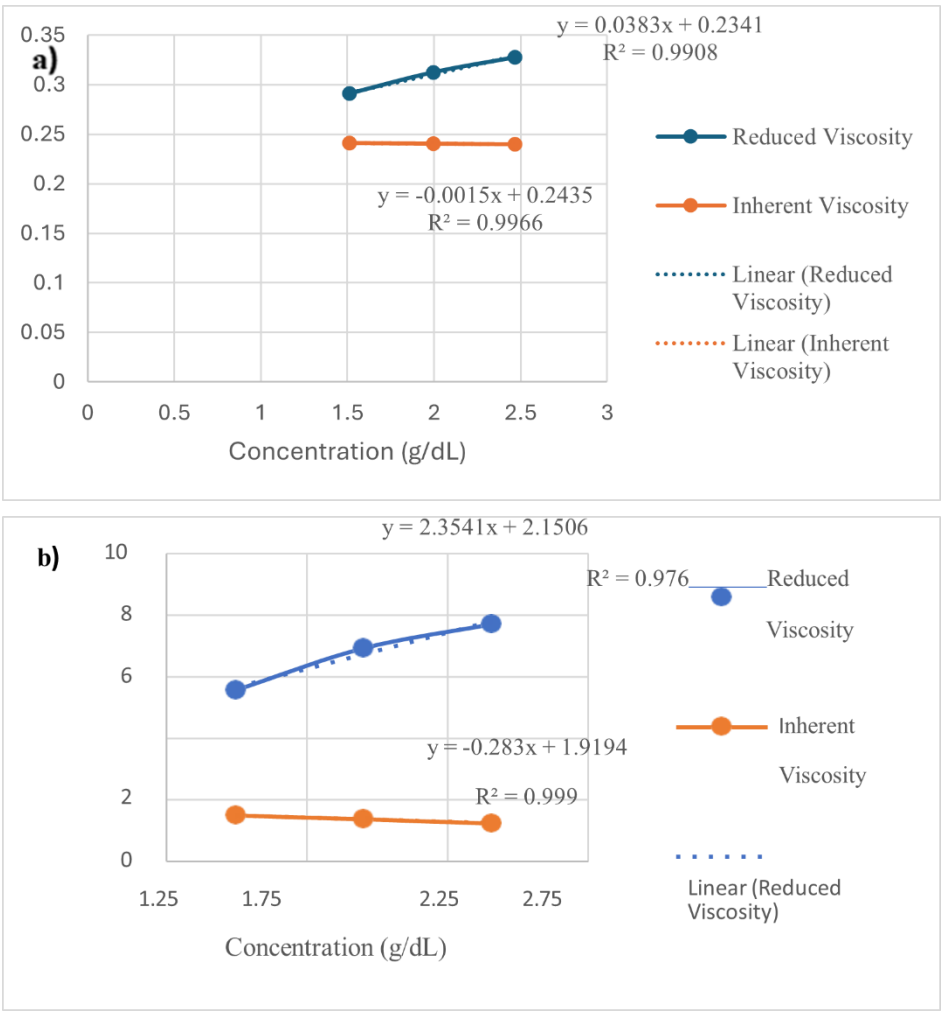

Figure 21: Viscometer data for (a) PML and (b) 3100 HP

Based on the intrinsic viscosity for PML it was deduced that M_v~13,402 g/mol in comparison to the control (3100 HP) whose M_v ~ 198,200 g/mol. As expected, poly(L-lactide)'s spectrum represents an isotactic structure (**Figure 22a**), as represented by the iii tetrad sequences (5.14-5.20 ppm), with ~90% monomer conversion. This indicates that the existing (S) asymmetric centers are completely retained during polymerization. In contrast, poly(meso-lactide)'s spectrum represents an atactic structure (**Figure 22b**) with >99% monomer conversion. This is characterized by the sis tetrad peaks between 5.2 to 5.3 ppm.

In addition, the original iii tetrad sequences from PLLA's spectrum transition to isi, iss, ssi, and sss tetrad configurational sequences. Pentad configurational sequences were assigned for the peaks based on Kaperczyk's analysis using HETCOR NMR, indicating a random statistical distribution of tetrad tacticity's [34].

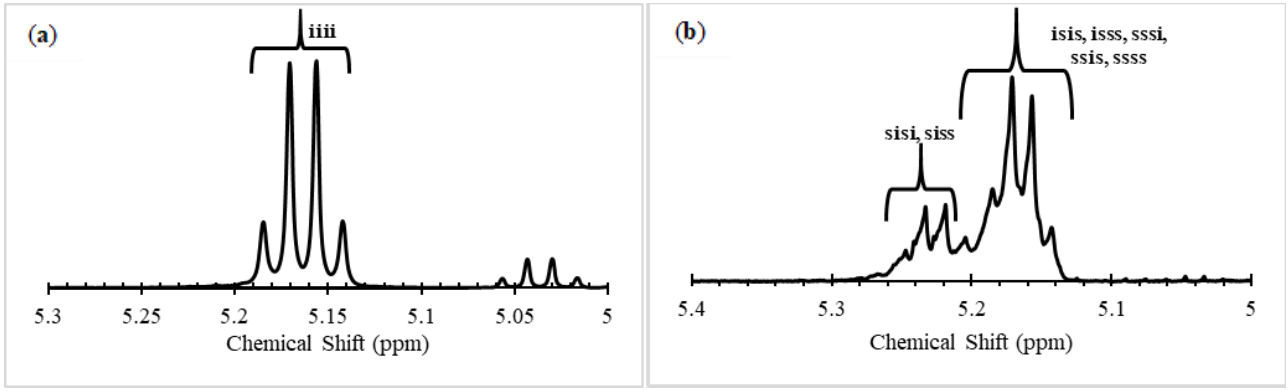

Figure 22: NMR spectra of (a) poly(L-lactide) and (b) poly(meso-lactide)

Modification of PML by VTMOS through free radical grafting was done in the Parr reactor. REX was utilized for modification of high molecular weight PLAs. Moving over the course REX would be adopted as it provides a facile and continuous method for scale up. Below represents the thermal and structural characteristics.

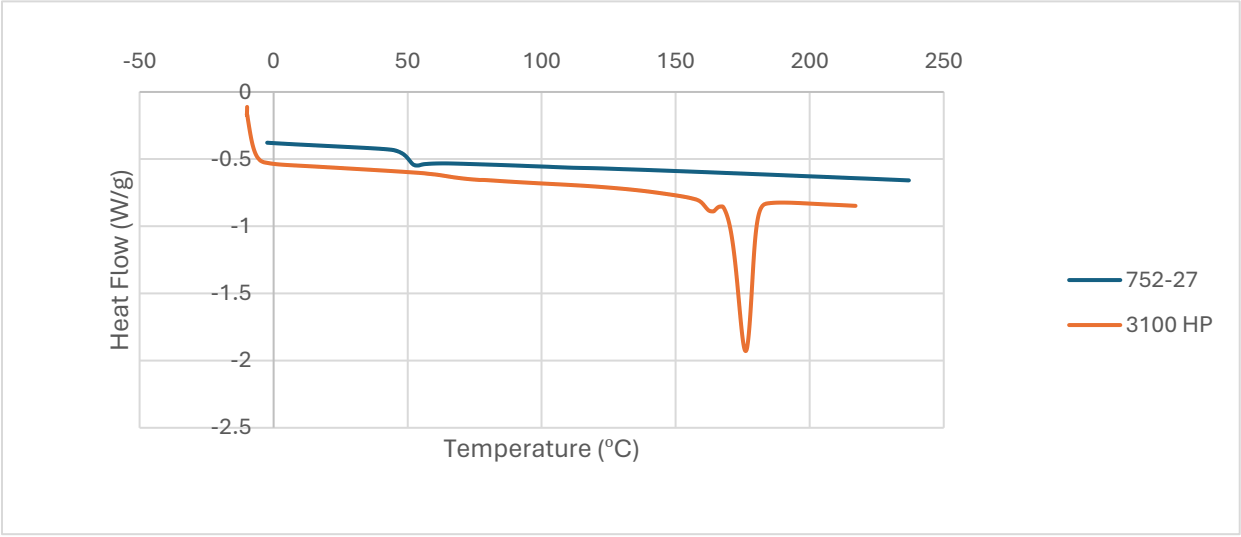

Figure 23: Thermal Properties of Modified PLAs

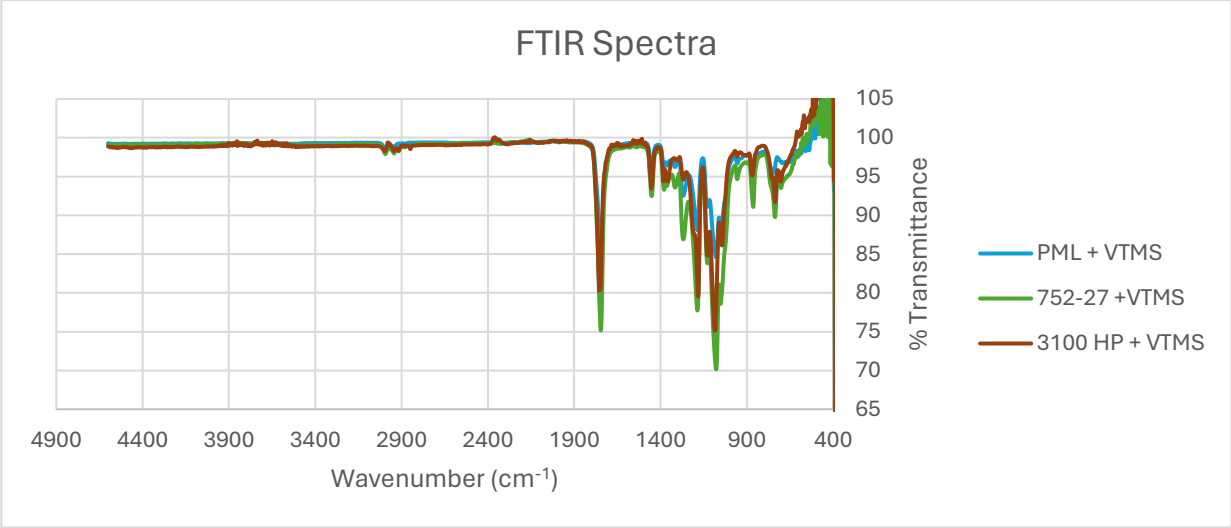

Figure 24: IR Spectra of Modified PLAs

No significant changes were observed in the melting temperature post modification. The VTMOS and PLA have a lot of overlapping peaks making a single discernable peak hard to identify. The sharp peak 752 is not present in PLA and represents the Si-C stretch in VTEOS. The decrease from 781 to 725-736 cm-1 is likely due to the radical trapping converting the Si-C=C bond to a Si-C-C bond.

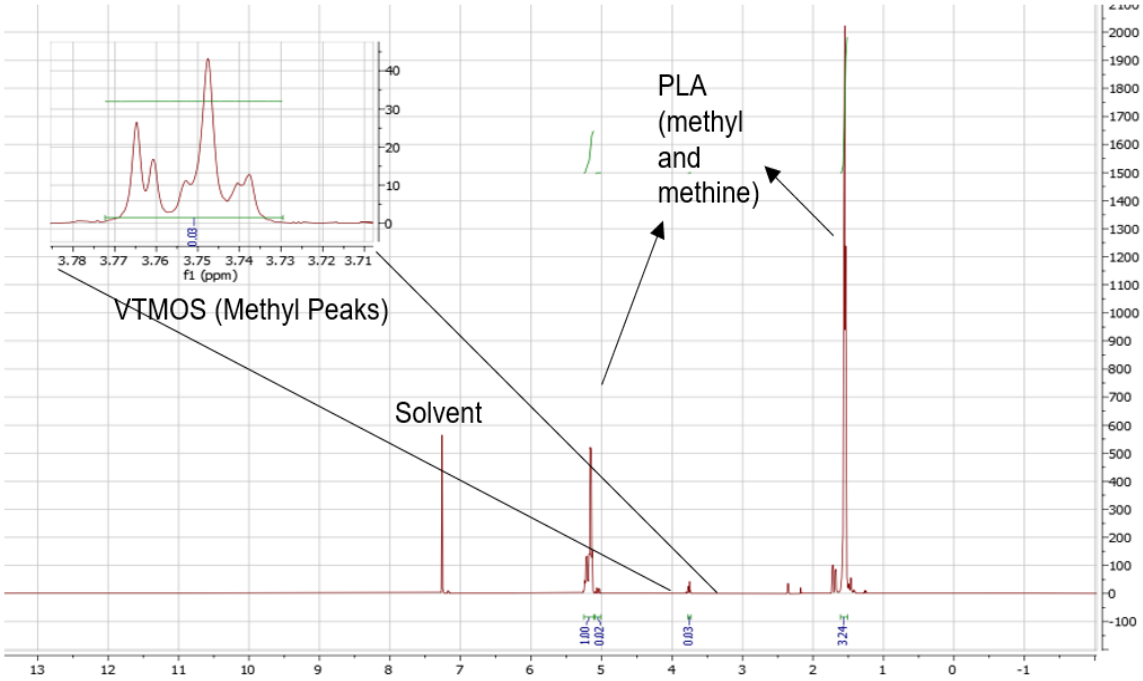

Figure 25: H^1 NMR OF PLA +VTMOS

H^1NMR was utilized for determining the % grafting of VTMOS.

$$\boldsymbol{VTMOS\ Weight}\ \% = \frac{\frac{\mathbf{1}}{\mathbf{9}} \times (\mathbf{148.23}) \times \int \boldsymbol{A}}{([\frac{\mathbf{1}}{\mathbf{9}} \times (\mathbf{148.23}) \times \int \boldsymbol{A}] + [\frac{\mathbf{1}}{\mathbf{3}} \times (\mathbf{72.06}) \times \int \boldsymbol{B}])} * \mathbf{100}$$

Here, A represents the integral area for methyl protons of VTMOS and B represents the methyl protons on the PLA backbone. Good integration agreement is found between the methyl and methine protons of PLA and for PML the % grafting was around 0.63 % weight. Similar calculations were performed on 752-27 and 3100 HP. It was observed around 0.3-0.4 wt.%. It is found that the bp of VTMOS is 120 ºC and the extrusion zone temperatures are higher which may cause evaporation and the initial input might deviate from 1 wt.% leading to lower% grafting for the REX process.

3.4 Conclusion and Next Steps

Meso-lactide was polymerized leading to an amorphous polymer as suggested by the DSC data. NMR alongside Polarimeter data showed a complete atactic structure with no optical activity. The reason for this structure change is most likely due to the random sequence of R and S units within the polymer chain. This atactic structure results in the polymer unable to pack into an ordered manner, which leads to an amorphous polymer.

Using FTIR and NMR, we were able to determine the % grafting of VTMOS onto PLA. Alternatively, using TGA to determine the % grafting and utilizing modified PLA for paper coating applications. Initial trials involving cobb value and grease resistance were tested utilizing roll coating method onto Kraft paper.

SYNTHESIS OF HIGH MOLECULAR WEIGHT POLYESTER VIA REX

4.1 Introduction and Background

In recent years there has been mounting interest in the use of "environmentally friendly" polymer materials that are biodegradable-compostable, recyclable, or derived from annually renewable resources [35]. Poly (ε-caprolactone) (PCL) and similar polyesters such as polylactides (PLA), poly hydroxyl butyrate (PHB), and poly hydroxy (butyrate-co-valerate) (PHBV) are biodegradable, and attention to their use in disposable short life single use packaging and consumer goods applications has been increasing [36][14]. This research involves reactive extrusion process for synthesizing three-arm poly (ε-caprolactone) using aluminum tri-sec butoxide (ATSB) as the initiator. It was further extrapolated to lactide (LA) for reactive extrusion polymerization of poly-lactide (PLLA). Extrusion Polymerization is a particular case of reactive extrusion that is conveniently implemented for synthesizing polymers in bulk (solvent-free) with global kinetics in order of minutes for complete conversion of monomer. This research involves reactive extrusion process for synthesizing three- arm poly (ε-caprolactone) using aluminum tri-sec butoxide (ATSB) as the initiator. Preliminary trials were conducted for reactive extrusion polymerization of lactide using stannous octoate (Sn $(Oct)_2$) and Triphenyl-phosphine ($P(Ph)_3$).

4.2 Experimental

4.2.1 Bulk Polymerization of ε-Caprolactone

Materials:

The CL monomer was used as received without any purification was designated ECL. CL monomer having 99.8% epsilon caprolactone content, 38 ppm or less of water, and 0.1 (mg of KOH/gm) or less acid value was designated ECL monomer and used in the study. The monomer is sourced from Ingevity, UK. A 97% pure ATSB initiator was obtained from Sigma Aldrich. A 5 wt.% solution of the initiator in anhydrous toluene (99.8% obtained from Aldrich) was prepared

and used for the polymerization. The monomer and the initiator solutions were stored under dry conditions in a nitrogen atmosphere. Extreme care was taken to prevent the entrainment of ambient moisture in any of the process steps, and the reaction was carried out under a dry nitrogen atmosphere.

Polymerization Chemistry

:

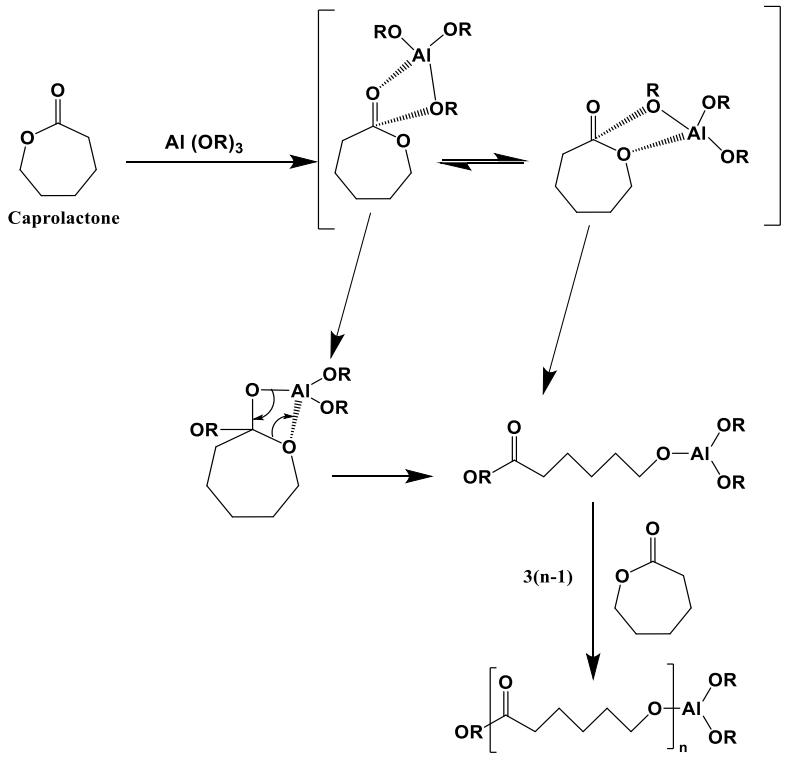

Figure 26: Coordination Insertion Mechanism of ε-Caprolactone polymerization

The ROP of ε-caprolactone occurs by a coordination-insertion mechanism in which the Al atom first coordinates with the carbonyl oxygen or the ring oxygen, followed by ring opening and insertion of the monomer between the Al atom and the alkoxides group as shown in Fig. 1. Using aluminum tri-alkoxides, three growing polyester chains are formed. Typically, workup of the solution polymerizations yields only linear polyester because of the hydrolysis of the Al-O bond.

However, we observe that under melt conditions and in the presence of shear, the three-arm polyester structure is retained, and the PCL product can be isolated (Fig. 21).

Reactive extrusion polymerization:

Reactive extrusion polymerization (REX) was conducted in co-rotating twin-screw extruder type ZSE 27 HP–PH from Leistritz (Nürnberg, Germany) as represented by the schematic in the below **Figure 27**. The screws used possess a diameter of 27 mm and an L/D ratio of about 40/1.

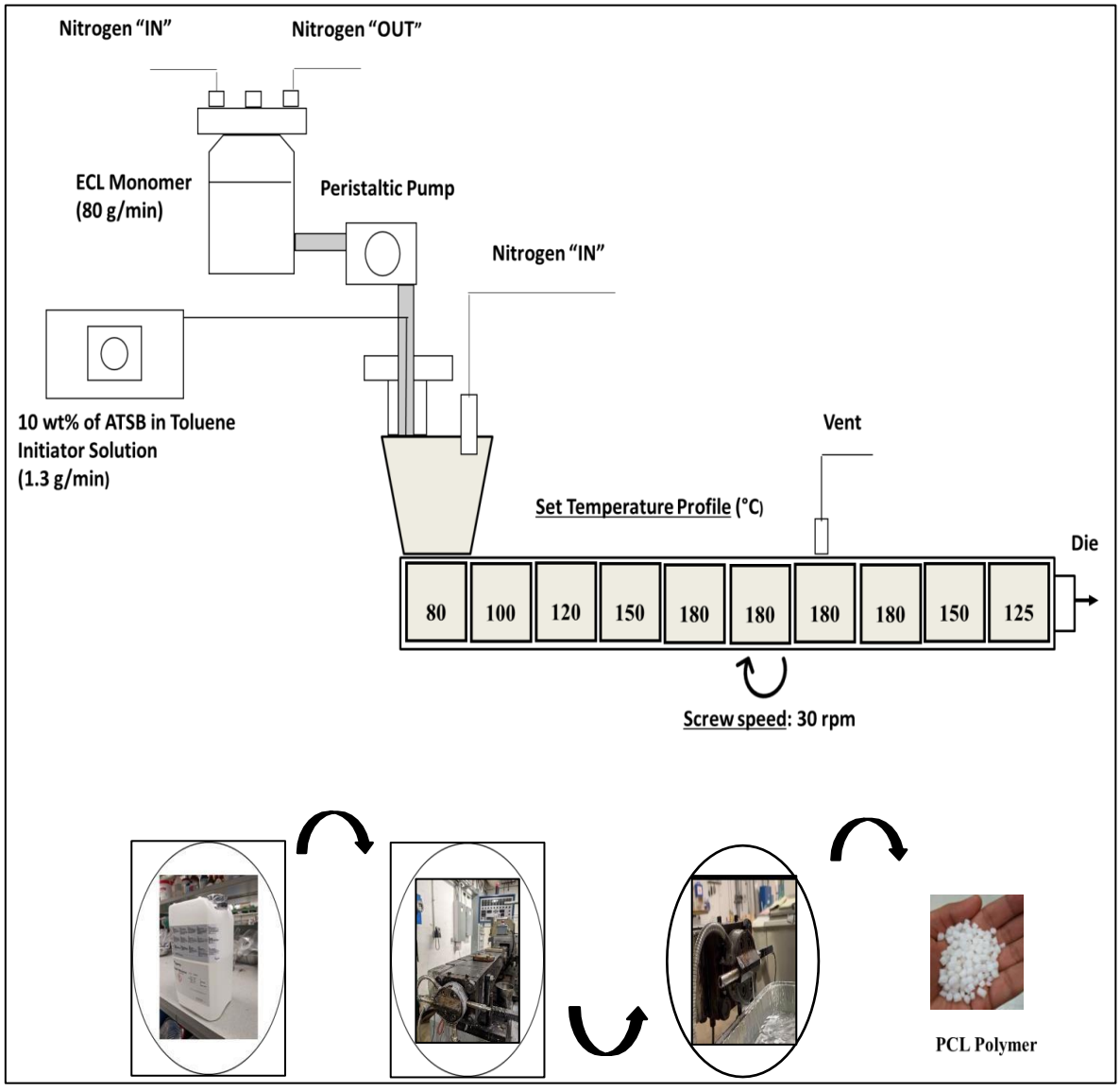

Figure 27: REX setup for Bulk Polymerization of ε-CL

Screw Configuration:

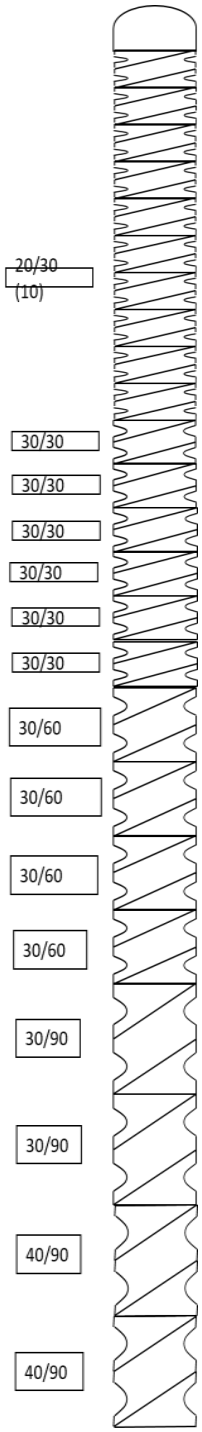

Figure 28: All conveying Screw Profile

All conveying screw profile was set on the extruder for maintaining forward conveying of liquid reagents for the polymerization. It also ensures sufficient residence time in the extruder (2-3 mins).

Characterization and analysis:

Thermal characterization of PCL was conducted using a DSC Q20 instrument to assess its thermal behavior. The testing procedure involved initial temperature equilibration at 0 ºC, followed by gradual heating to 180ºC at a rate of 10 ºC/min. This temperature was maintained isothermally for 5 minutes. Subsequently, the sample was cooled back to 0ºC at the same rate, and a 2-minute isothermal hold was performed. Finally, the material was reheated to 180ºC at 10 ºC/min.

The decomposition temperature and percentage weight loss were quantified using a thermogravimetric analyzer (TGA), specifically the TGA Q50. About 10 mg of sample was heated from 25 to 550°C at 20 ºC/min.

Viscosity is dependent on molecular weight distribution; correlations have been made between dilute solution viscosity and molecular weight. The ASTM D2857-16: Standard Practice for Dilute Solution Viscosity of Polymers and Intrinsic Viscosity of Polymer and Biopolymers Measured by Microchip has been referenced for the following procedure of viscosity and molecular weight determination. A constant-volume viscometer was used inside a fume hood operating at 27°C for all trials. The primary viscometer used was Canon 0C-D290. For one polymer sample, four trial concentrations were made by adding the required sample weight (mg) to a vial of 15ml of chloroform. The trial concentration in the vial was poured through a funnel into the viscometer. The sample was plunged up into the viscometer with a syringe. Using a stopwatch, the solution's passage through the marked region of the viscometer was timed to obtain an efflux time. This was repeated three times for each sample concentration and pure solvent sample. The average of the sample efflux times was used in viscosity calculations.

4.3 Results and Discussion

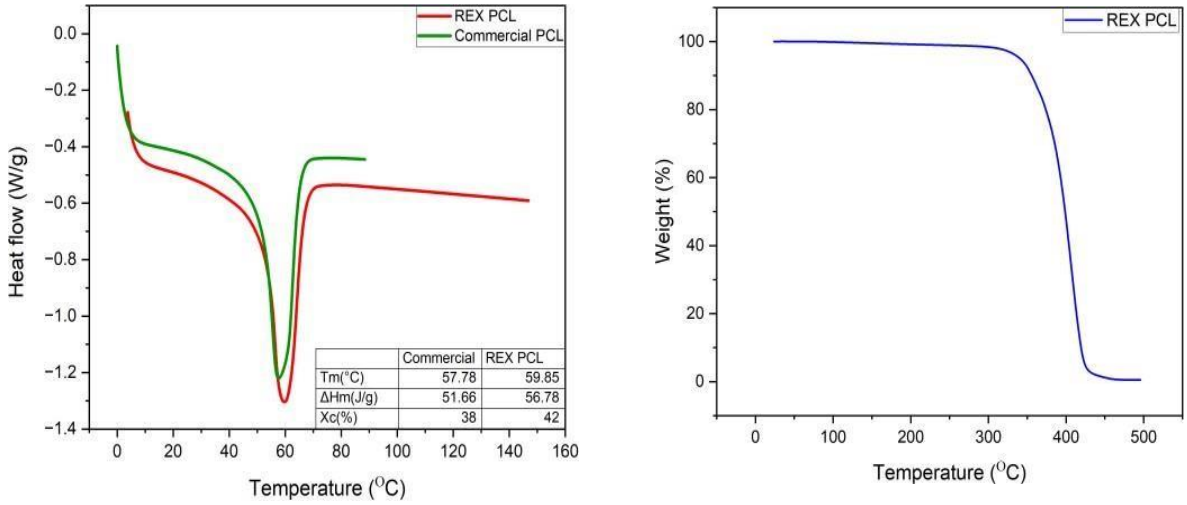

Figure 29: Thermal Properties of PCL and Commercial PCL

Figure 29, DSC showed peak melting temperature at 60 ºC and was compared against commercial PCL. Peak degradation temperature around 372 ºC was observed. In **Figure 30**, intrinsic viscosity of three-arm PCL was calculated to be 1.275 dL/g.

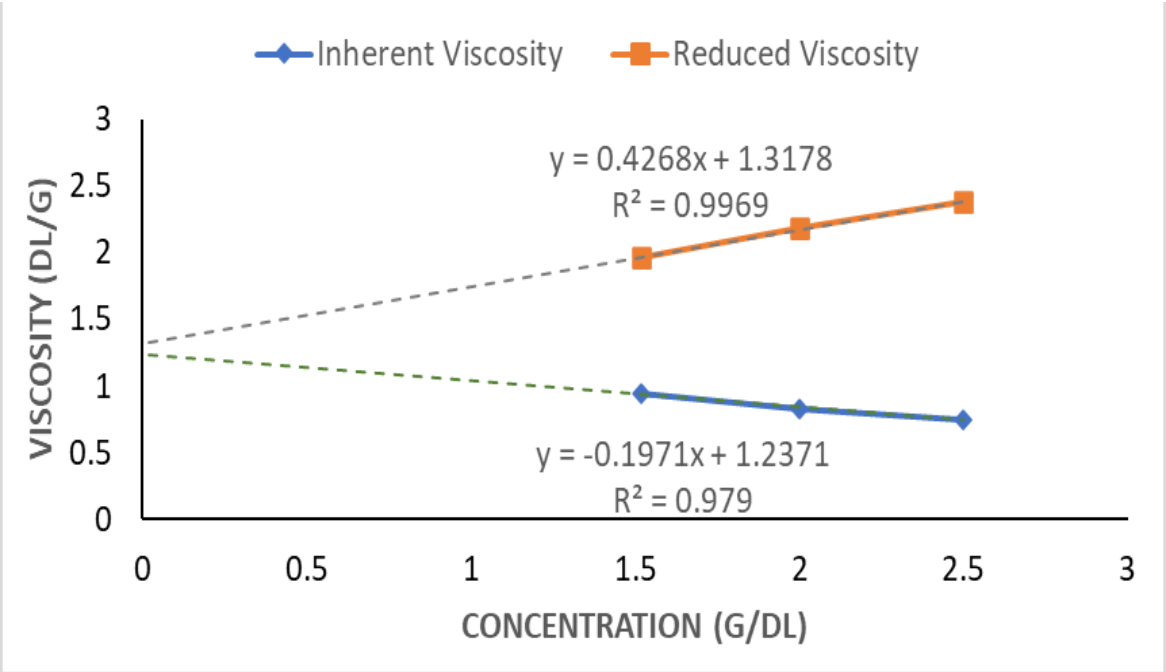

Figure 30: Solution Viscometry of PCL

4.4 Conclusion and Next Steps

Three-arm PCL was continuously synthesized using REX and further elucidating the three-arm structure.

Preliminary trials for L-lactide polymerization were conducted. The materials were purchased from Aldrich. L-lactide was kindly provided by Total Corbion (Lumilact-l). The chemistry was similar, as described in the previous chapter. The extrusion setup was similar as for PCL except there was one gravimetric feeder for solid feeding of the lactide flakes. Results showed M_v~ 40,000 g/mol of PLLA.

Future studies delve into utilization of REX for synthesizing high molecular weight polyester and co-polyester.

BIBLIOGRAPHY

[1] Neufeld, L., et al. The new plastics economy: rethinking the future of plastics. in the World Economic Forum. 2016.

[2] L. Lebreton, A. Andrady, Future scenarios of global plastic waste generation and disposal, Palgrave Commun. 5 (2019) 6. https://doi.org/10.1057/s41599-018-0212-7.

[3] J. Zalasiewicz, S. Gabbott, C.N. Waters, Chapter 23 - Plastic Waste: How Plastics Have Become Part of the Earth's Geological Cycle, in: T.M. Letcher, D.A.B.T.-W. (Second E. Vallero (Eds.), Academic Press, 2019: pp. 443–452. https://doi.org/https://doi.org/10.1016/B978-0-12-815060-3.00023-2.

[4] J.R. Jambeck, R. Geyer, C. Wilcox, T.R. Siegler, M. Perryman, A. Andrady, R. Narayan, K.L. Law, Plastic waste inputs from land into the ocean, Science (80-.). 347 (2015) 768– 771. https://doi.org/10.1126/science.1260352.

[5] M.C. Rillig, Microplastic in terrestrial ecosystems and the soil, Environ. Sci. Technol. 46 (2012) 6453–6454. https://doi.org/10.1021/es302011r.

[6] J. Lunt, Large-scale production, properties and commercial applications of polylactic acid polymers, Polym. Degrad. Stab. 59 (1998) 145–152.https://doi.org/https://doi.org/10.1016/S0141-3910(97)00148-1.

[7] R.E. Drumright, P.R. Gruber, D.E. Henton, Polylactic Acid Technology, Adv. Mater. 12 (2000) 1841–1846. https://doi.org/https://doi.org/10.1002/1521- 4095(200012) 12:23<1841::AID-ADMA1841>3.0.CO;2-E.

[8] D. Garlotta, A Literature Review of Poly (Lactic Acid), J. Polym. Environ. 9 (2001) 63–84. https://doi.org/10.1023/A:1020200822435.

[9] R. Auras, Poly (lactic acid), in: Encycl. Polym. Sci. Technol., 2010. https://doi.org/https://doi.org/10.1002/0471440264.pst275.

[10] P. Giri, C. Tambe, R. Narayan, Using Reactive Extrusion To Manufacture Greener Products: From Laboratory Fundamentals to Commercial Scale, in: Biomass Extrus. React. Technol. Princ. to Pract. Futur. Potential, American Chemical Society, 2018: p. 1. https://doi.org/doi:10.1021/bk-2018-1304.ch001.

[11] P. Dubois, R. Narayan, Biodegradable compositions by reactive processing of aliphatic polyester/polysaccharide blends, Macromol. Symp. 198 (2003) 233–244. https://doi.org/https://doi.org/10.1002/masy.200350820.

[12] C. Tzoganakis, Reactive extrusion of polymers: A review, Adv. Polym. Technol. 9 (1989) 321–330. https://doi.org/https://doi.org/10.1002/adv.1989.060090406.

[13] D.E. Crawford, Extrusion – back to the future: Using an established technique to reform automated chemical synthesis, Beilstein J. Org. Chem. 13 (2017) 65–75. https://doi.org/10.3762/bjoc.13.9.

[14] J.-M. Raquez, P. Degée, Y. Nabar, R. Narayan, P. Dubois, Biodegradable materials by reactive extrusion: from catalyzed polymerization to functionalization and blend compatibilization, Comptes Rendus Chim. 9 (2006) 1370–1379. https://doi.org/https://doi.org/10.1016/j.crci.2006.09.004.

[15] H. Tsuji, Poly(lactide) Stereocomplexes: Formation, Structure, Properties, Degradation, and Applications, Macromol. Biosci. 5 (2005) 569–597. https://doi.org/https://doi.org/10.1002/mabi.200500062.

[16] H. Tsuji, Y. Ikada, Stereocomplex formation between enantiomeric poly(lactic acid)s. XI. Mechanical properties and morphology of solution-cast films, Polymer (Guildf). 40 (1999) 6699–6708. https://doi.org/https://doi.org/10.1016/S0032-3861(99)00004-X.

[17] H. Tsuji, Y. Ikada, Crystallization from the melt of poly(lactide)s with different optical purities and their blends, Macromol. Chem. Phys. 197 (1996) 3483–3499. https://doi.org/https://doi.org/10.1002/macp.1996.021971033.

[18] Z. JM, H. Sato, H. Tsuji, I. Noda, Y. Ozaki, Infrared spectroscopic study of CH3 center dot center dot center dot O=C interaction during poly(L-lactide)/poly(D-lactide) stereocomplex formation, Macromolecules. 38 (2005) 1822–1828. https://doi.org/10.1021/ma047872w.

[19] M. Alhaj, R. Narayan, Scalable Continuous Manufacturing Process of Stereocomplex PLA by Twin-Screw Extrusion, Polymers (Basel). 15 (2023). https://doi.org/10.3390/polym15040922.

[20] X. Su, L. Feng, D. Yu, Formation of Stereocomplex Crystal and Its Effect on the Morphology and Property of PDLA/PLLA Blends, Polymers (Basel). 12 (2020). https://doi.org/10.3390/polym12112515.

[21] Q. Xie, L. Han, G. Shan, Y. Bao, P. Pan, Polymorphic Crystalline Structure and Crystal Morphology of Enantiomeric Poly(lactic acid) Blends Tailored by a Self-Assemblable Aryl Amide Nucleator, ACS Sustain. Chem. Eng. 4 (2016) 2680–2688. https://doi.org/10.1021/acssuschemeng.6b00191.

[22] S. Körber, K. Moser, J. Diemert, Development of High Temperature Resistant Stereocomplex PLA for Injection Moulding, Polymers (Basel). 14 (2022). https://doi.org/10.3390/polym14030384.

[23] A. Gupta, N. Mulchandani, M. Shah, S. Kumar, V. Katiyar, Functionalized chitosan mediated stereocomplexation of poly(lactic acid): Influence on crystallization, oxygen permeability, wettability and biocompatibility behavior, Polymer (Guildf). 142 (2018) 196–208. https://doi.org/https://doi.org/10.1016/j.polymer.2017.12.064.

[24] J. Jeong, M. Ayyoob, J.-H. Kim, S.W. Nam, Y.J. Kim, In situ formation of PLA-grafted alkoxysilanes for toughening a biodegradable PLA stereocomplex thin film, RSC Adv. 9 (2019) 21748–21759. https://doi.org/10.1039/C9RA03299A.

[25] D. Gregor-Svetec, T. Šumrada, Packaging paper coated with PLA, 2020. https://doi.org/10.24867/GRID-2020-p33.

[26] K. Khwaldia, E. Arab-Tehrany, S. Desobry, Biopolymer Coatings on Paper Packaging Materials, Compr. Rev. Food Sci. Food Saf. 9 (2010) 82–91. https://doi.org/https://doi.org/10.1111/j.1541-4337.2009.00095.x.

[27] A. Nair, D. Kansal, A. Khan, M. Rabnawaz, Oil- and water-resistant paper substrate using blends of chitosan-graft-polydimethylsiloxane and poly(vinyl alcohol), J. Appl. Polym. Sci. 138 (2021) 50494. https://doi.org/https://doi.org/10.1002/app.50494.

[28] S.S. Hamdani, Z. Li, E. Rolland, M. Mohiuddin, M. Rabnawaz, Barrier and mechanical properties of biodegradable paper bilayer-coated with plasticized starch and zein, J. Appl. Polym. Sci. 140 (2023) e53440. https://doi.org/https://doi.org/10.1002/app.53440.

[29] V.K. Rastogi, P. Samyn, Bio-Based Coatings for Paper Applications, Coatings. 5 (2015) 887–930. https://doi.org/10.3390/coatings5040887.

[30] M. Ryner, K. Stridsberg, A.-C. Albertsson, H. von Schenck, M. Svensson, Mechanism of Ring-Opening Polymerization of 1,5-Dioxepan-2-one and l-Lactide with Stannous 2-Ethylhexanoate. A Theoretical Study, Macromolecules. 34 (2001) 3877–3881. https://doi.org/10.1021/ma002096n.

[31] D. Pholharn, Y. Srithep, J. Morris, Effect of initiators on synthesis of poly(L-lactide) by ring opening polymerization, IOP Conf. Ser. Mater. Sci. Eng. 213 (2017) 12022. https://doi.org/10.1088/1757-899X/213/1/012022.

[32] J. Schneider, Moisture curable toughened poly(lactide) utilizing vinyltrimethoxysilane based crosslinks, Express Polym. Lett. 10 (2016) 799–809. https://doi.org/10.3144/expresspolymlett.2016.75.

[33] M. Avella, M.E. Errico, B. Immirzi, M. Malinconico, E. Martuscelli, L. Paolillo, L. Falcigno, Radical polymerization of poly(butyl acrylate) in the presence of poly(L-lactic acid), 1. Synthesis, characterization and properties of blends, Die Angew. Makromol. Chemie. 246 (1997) 49–63. https://doi.org/https://doi.org/10.1002/apmc.1997.052460104.

[34] J.E. Kasperczyk, HETCOR NMR study of poly(rac-lactide) and poly(meso-lactide), Polymer (Guildf). 40 (1999) 5455–5458. https://doi.org/https://doi.org/10.1016/S0032-3861(99)00128-7.

[35] J.-M. Raquez, P. Degee, P. Dubois, S. Balakrishnan, R. Narayan, Melt-stable poly (1,4-dioxan-2-one) (co)polymers by ring-opening polymerization via continuous reactive extrusion, Polym. Eng. Sci. 45 (2005) 622–629. https://doi.org/https://doi.org/10.1002/pen.20312.

[36] S. Balakrishnan, M. Krishnan, R. Narayan, P. Dubois, Three-arm poly (ε-caprolactone) by extrusion polymerization, Polym. Eng. Sci. 46 (2006) 235–240. https://doi.org/https://doi.org/10.1002/pen.20344.